CAMBRIDGE

ILLUSTRATED

HANDBOOK OF OPTOELECTRONICS AND PHOTONICS

SAFA KASAP, HARRY RUDA
AND YANN BOUCHER

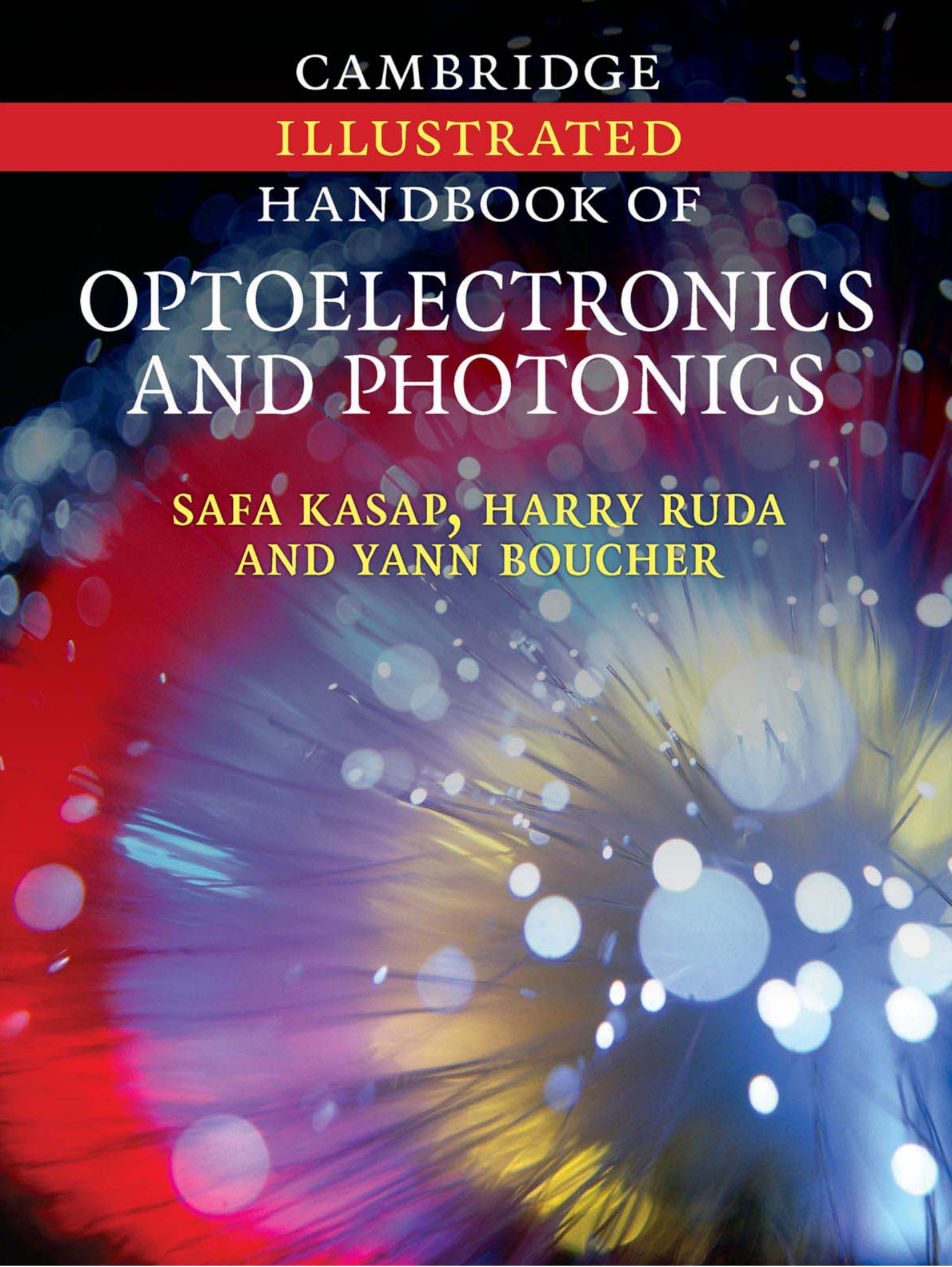

Cambridge Illustrated Handbook of Optoelectronics and Photonics

Safa Kasap
University of Saskatchewan, Canada

Harry Ruda
University of Toronto, Canada

Yann Boucher
École Nationale d'Ingénieurs de Brest, France

CAMBRIDGE
UNIVERSITY PRESS

CAMBRIDGE UNIVERSITY PRESS
Cambridge, New York, Melbourne, Madrid, Cape Town, Singapore, São Paulo, Delhi

Cambridge University Press
The Edinburgh Building, Cambridge CB2 8RU, UK

Published in the United States of America by Cambridge University Press, New York

www.cambridge.org
Information on this title: www.cambridge.org/9780521815963

First published 2009

Printed in the United Kingdom at the University Press, Cambridge

A catalog record for this publication is available from the British Library

Library of Congress Cataloguing in Publication data
Kasap, S. O. (Safa O.)
Cambridge illustrated handbook of optoelectronics and photonics : an illustrated encyclopedic dictionary of significant terms, effects, phenomena, equations, and properties, from fundamental concepts to applications, from materials to devices to systems, covering optoelectronics and photonics, including optical communications / Safa
Kasap, Harry Ruda, Yann G. Boucher.
p. cm.
ISBN 978-0-521-81596-3 (hardback)
1. Optoelectronics – Encyclopedias. 2. Optoelectronic devices – Encyclopedias.
I. Ruda, Harry E., 1958– II. Boucher, Yann G. III. Title.
TA1750.K383 2009
621.381′045 – dc22 2008045090

ISBN 978-0-521-81596-3 hardback

Preface

The present work is an illustrated encyclopedic handbook of important terms and effects from fundamental concepts to applications in optoelectronics and photonics, including optical communications. We tried to define and describe terms from materials to devices to systems, as photonics is still in its early stages of evolution compared with microelectronics and today's billion-transistor chips, and systems on chips. It is *not* meant to be a comprehensive encyclopedia or a dictionary in this field but rather a self-contained semiquantitative description of terms and effects that frequently turn up in optoelectronics and photonics courses at the undergraduate and graduate levels. There is nothing worse than a dry reference book with no illustrations. We prepared numerous illustrations to convey the message as clearly as possible. There is an old Chinese adage that a good diagram is worth a thousand words but a bad diagram takes a thousand words to explain. Nearly all the illustrations have been prepared almost from scratch to be as self-explanatory and as clear as possible. In writing such an *encyclopedic handbook* we had to choose between short and quick definitions and definitions that encompass an extensive explanation; the choice was based on whether a term can be defined simply and still be useful, e.g. the acceptance cone of a fiber, or whether the term needs at least one page of explanations to be fair to the term and the reader, e.g. photonic crystals. In addition, we had to draw a distinction between an optics handbook and what we had in mind as a useful encyclopedic handbook for optoelectronics and photonics. We have missed many terms but we have also described many, through, undoubtedly, our own biased selection. In our own view there is not a huge difference between optoelectronics and photonics, except that in the latter there may not be any electronics involved. Today, photonics is a more fashionable term than the old optoelectronics term which usually conjures images of LEDs, solar cells, optoisolators, etc., whereas photonics is closely associated with optical communications and optical signal processing. True photonics is supposed to be a subject based on photons, or electromagnetic radiation, only; but, in practice, it is impossible to avoid electrons when photons have to be generated or detected.

"After a year's research one realises that it could have been done in a week"

Sir William Henry Bragg (1862–1942)

Numerical definitions

1/*f* noise see *excess noise*.

10Dq see *ligand field splitting parameter*.

1.24 "rule" is the equation that is widely used in converting between the photon energy E in eV and the radiation wavelength λ in microns: $\lambda(\mu\text{m}) = 1.24[E(\text{eV})]^{-1}$. It arises from $E = h\nu = hc/\lambda$.

A

Abbe condenser is a high numerical aperture lens system that normally has two lenses designed to collect and suitably direct light to an object that is to be examined in a microscope.

Abbe diagram see *Abbe number*.

Abbe number or **constringence** of an optical medium is the inverse of its *dispersive power*, that is, it represents the relative importance of refraction and dispersion. There are two common definitions based on using different standard wavelengths. The Abbe number v_d is defined by

$$v_d = (n_d - 1)/(n_F - n_C)$$

where n_F, n_d and n_C are the refractive indices of the medium at the Fraunhofer standard wavelengths corresponding to the helium d-line ($\lambda_d = 587.6$ nm, yellow), hydrogen F-line ($\lambda_F = 486.1$ nm, blue) and hydrogen C-line ($\lambda_C = 656.3$ nm, red). The Abbe number v_e, on the other hand, is defined by

$$v_e = (n_e - 1)/(n_{F'} - n_{C'})$$

where n_e, $n_{F'}$ and $n_{C'}$ are refractive indices at the e-line (546.07 nm), F'-line (479.99 nm) and C'-line (643.85 nm) wavelengths respectively.

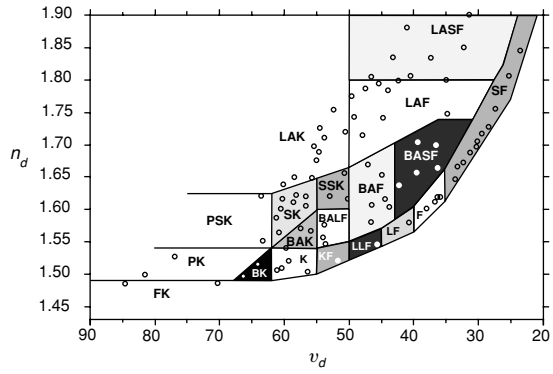

Abbe number The *Abbe diagram* is a diagram in which the refractive index n_d of glasses are plotted against their Abbe numbers in a linear n_d vs. v_d plot and, usually, with the Abbe number decreasing along the x-axis, rather than increasing (v_d values on the the x-axis have been reversed). The last letter F or K represents flint or crown glass. Other symbols are as follows: S, dense; L, light; LL, extra light; B, borosilicate; P, phosphate; LA or La, lanthanum; BA or Ba, barium. Examples: BK, dense flint; LF, light flint; LLF, extra light flint; SSK, extra dense crown; PK, phosphate crown; BAK, barium crown; LAF, lanthanum flint, etc. (Adapted from Schott Glass Website.) See *chromatic dispersion*.

Table: Abbe number PC is polycarbonate, PMMA is polymethylmethacrylate, PS is polystyrene.

Optical glass	SF11	F2	BaK1	crown glass	fused silica	PC	PMMA	PS
v_d	25.76	36.37	57.55	58.55	67.8	34	57	31

[Sources: Melles-Griot and Goodfellow websites]

Abbe-Porro prism is a prism that transmits the image through the prism laterally displaced but fully inverted, that is, flipped vertically and horizontally. It is very similar in its function to the double Porro prism. See *Porro prism*.

Abbe prism is a reflection prism that uses reflections rather than refractions to deflect (deviate) light, invert or rotate an image.

Abbe refractometer see *refractometer*.

Abbe's sine condition, discovered by Abbe and Helmholtz (1873) and also simply called the *sine condition*, specifies the condition under which arbitrary rays leaving a particular point P_o on the object are able to arrive at the same (and unique) image point P_i that is an image (or conjugate point) of P_o. Consider an image formed by a spherical surface. A point P_o on the object at a height y_o in the object space of refractive index n_o gives rise to a point P_i of height y_i in the image space of index n_i; the two media are separated by a spherical boundary with its center of curvature at C. An arbitrary ray from P_o that is incident on the spherical surface at A (an arbitrary point) is refracted, and can only pass through the required unique image point P_i if *Abbe's sine* condition is satisfied, i.e.

$$n_o y_o \sin\theta_o = n_i y_i \sin\theta_i$$

where θ_o is the angle the object ray P_oA makes with the principal ray P_oCP_i (that ray passing through the center C without refraction) and θ_i is the angle that the image ray AP_i makes with the principal ray P_oCP_i. There are no assumptions in this condition, and if an optical system is such that it satisfies the sine condition, then spherical and coma (off-axis) aberrations are eliminated since all arbitrary rays from P_o arrive at P_i. Consider a simple lens imaging system in which the object and the image are in the same refractive index media, $n_o = n_i$. The magnification is y_o/y_i, so that $y_i/y_o = \sin\theta_o/\sin\theta_i$. Both marginal and paraxial rays will produce the same magnification, that is the same P_i for a given P_o, if

$$y_i/y_o = \sin\theta_o/\sin\theta_i = \theta_{op}/\theta_{ip} = \text{constant}$$

which will then result in no spherical or coma aberration; $\sin\theta_o/\sin\theta_i = \theta_{op}/\theta_{ip}$ is sometimes stated as the *sine condition* for the absence of spherical and coma aberration. It has been stated that "Abbe's sine condition requires that all rays emanating from the axial object point within the incident cone must emerge in image space, where they form a converging cone toward the axial image point, at the same height at which they entered the system" (M. Born and E. Wolf, *Principles of Optics*, Cambridge University Press, 1999). The height OA must be the same for both the object rays and the image rays. See *aplanaticlens, aplanatic optical system, aplanatic points*.

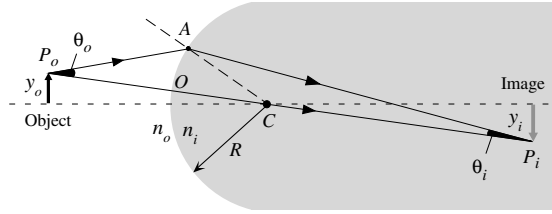

Abbe's sine condition for refraction at a curved surface. C is the center of curvature. Subscripts o and i refer to object and image.

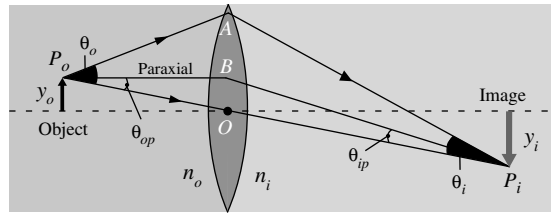

Abbe's sine condition for a lens; an arbitrary ray from P_o generates P_i.

Abbe's theory of microscope imaging refers to the case where the (thin) *phase object* is under coherent illumination, either by a laser or by light emitted from a sufficiently small source via a condenser of low aperture. The object in the Π plane acts as a diffraction phase grating, forming its

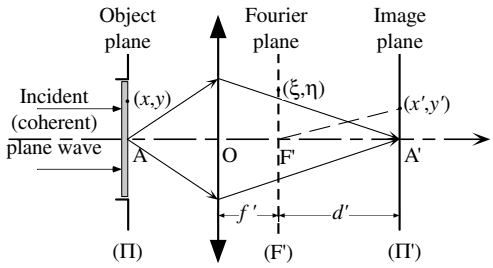

Abbe's theory of image formation. A filter conveniently located in the F′ plane enables one to select, or suppress, any given spatial frequency. (x,y) represent the coordinates of a point on the object plane, (ξ,η) the coordinates of a point on the Fourier transform plane, and (x',y') the coordinates of a point on the image plane. See also *spatial filtering*.

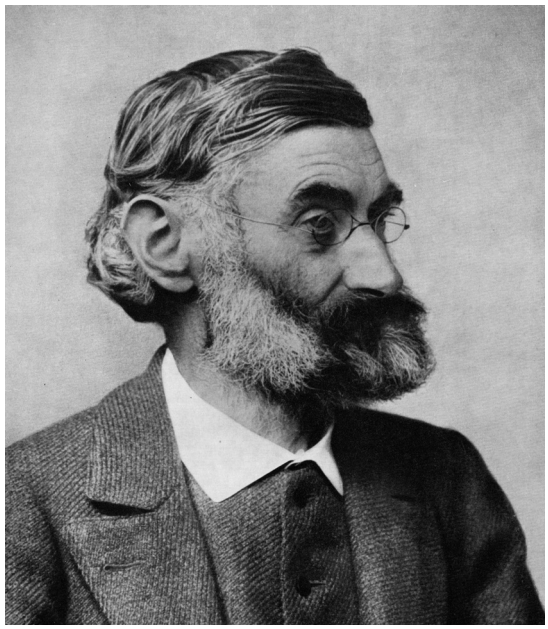

Ernst Abbe (1840–1905, Germany). Ernst Abbe was appointed a professor of physics and mathematics at Jena in 1870. As a result of his innovative works on optics with Carl Zeiss, Abbe became quite wealthy. (Jena Review, 1965, Zeiss Archive, courtesy AIP Emilio Segre Visual Archives, E. Scott Barr Collection.)

Fourier transform in the image focal plane F′ of the objective, where each point acts as a secondary source. The final image in the image plane Π′ is the result of the interference of all these sources. The whole theory has been summarized as follows: "The microscope image is the interference effect of diffraction phenomena."

ABCD matrix or **ray-transfer matrix** is a matrix that conveniently describes an optical operation on a ray of light; it is a direct result of the linearity of the paraxial equations. At any abscissa z along the main axis, any given optical ray propagating in a medium of refractive index n is completely determined by two numbers: the distance $\rho(z)$ to the axis and the reduced slope $\theta(z) = n(z)d\rho(z)/dz$ as illustrated in the figure.

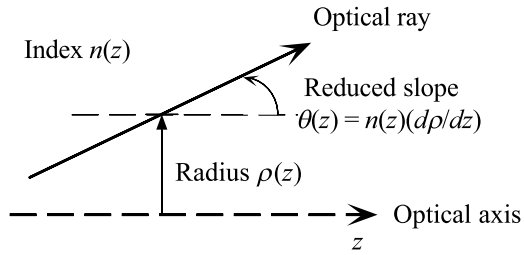

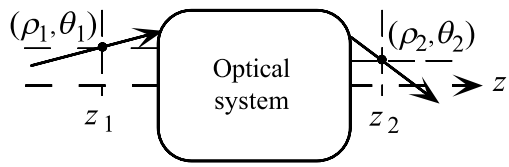

The couple $\{\rho_1,\theta_1\}$ at abscissa z_1 is transformed at abscissa z_2 into $\{\rho_2,\theta_2\}$ such that

$$\begin{pmatrix}\rho_2\\ \theta_2\end{pmatrix} = \begin{pmatrix}A & B\\ C & D\end{pmatrix}\begin{pmatrix}\rho_1\\ \theta_1\end{pmatrix},$$

with $AD-BC=1$. Some examples are reported in the following table.

Propagation in free space (length L, index n_0)	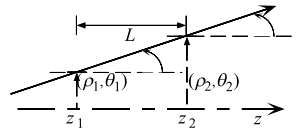	$\begin{pmatrix}\rho_2\\ \theta_2\end{pmatrix} = \begin{pmatrix}1 & L/n_0\\ 0 & 1\end{pmatrix}\begin{pmatrix}\rho_1\\ \theta_1\end{pmatrix}$
Thin lens (focal f)	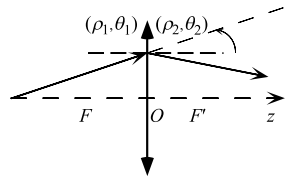	$\begin{pmatrix}\rho_2\\ \theta_2\end{pmatrix} = \begin{pmatrix}1 & 0\\ -1/f & 1\end{pmatrix}\begin{pmatrix}\rho_1\\ \theta_1\end{pmatrix}$

Any succession of optical elements, all aligned along a single axis, can therefore be associated a single ray-transfer matrix, obtained by a matrix product (in the right order) of each subcomponent. This can be successfully generalized to a linear medium exhibiting a refractive index decreasing quadratically with ρ, such as $n(\rho) = n_0(1-\gamma^2\rho^2/2)$. In this case,

$$\begin{pmatrix}\rho_2\\ \theta_2\end{pmatrix} = \begin{pmatrix}\cos(\gamma z) & \sin(\gamma z)/(n_0\gamma)\\ -(n_0\gamma)\sin(\gamma z) & \cos(\gamma z)\end{pmatrix}\begin{pmatrix}\rho_1\\ \theta_1\end{pmatrix},$$

and the optical ray is "trapped" along the axis, forced to propagate in a curved way. Graded-index quadratic fibers are based on this principle (GRIN fibers).

Two other applications of ABCD matrices should be mentioned: the stability analysis of laser cavities and the propagation of Gaussian beams generated by such a laser.

Aberrations generally refer to unwanted deviations in the optical imaging characteristics of a lens or a mirror from the ideal, based on *paraxial ray imaging*. Aberrations are usually divided into two categories. *Chromatic aberration* is due to the wavelength dependence of the refractive index and hence the focal length f, which now depends on the color of light. *Monochromatic* (or near monochromatic) *aberrations* are also called *third-order aberrations* (originally analyzed by Seidel in 1857) and are primarily *spherical*, *coma*, *astigmatism*, *field curvature*, and *distortion*, and arise as a result of the departure from the paraxial approximation when the angles of the rays in the imaging system are not sufficiently small. Aberrations typically result in the distortions of the image and in the unwanted blurring in the image quality (loss of resolution). When a light ray traveling in air is incident on a lens, it is refracted at the lens surface. It obeys Snell's law, i.e.

$$n_1 \sin\theta_1 = n_2 \sin\theta_2$$

where n_1 and n_2 are the air and glass (lens) refractive indices and θ_1 and θ_2 are the angles of incidence and refraction with respect to the normal on the lens surface at the point of incidence. There is a similar expression for the ray leaving the lens. The whole paraxial lens theory and the usual lens equations are based on assuming small angles so that $\sin\theta_1 \approx \theta_1$, and $\sin\theta_2 \approx \theta_2$, and $n_1\theta_1 \approx n_2\theta_2$. Thus, in

$$\sin\theta = \theta - \frac{\theta^3}{3!} + \frac{5^3}{5!} - \ldots$$

we normally neglect the third-order and higher terms, which is the paraxial approximation; small angles. The third-order term $(\theta^3/3!)$ is the cause of third-order aberrations, which are sometimes called *Seidel aberrations*. Unless $\theta = 0$ (normal incidence), there will always be a third term in the above expansion (small but finite), and hence always some aberration. In practice, aberrations occur in combination which makes it difficult to cancel them exactly. Nonetheless, either by suitable lens shaping, or using two or more lenses with stops,

Table: Aberrations in optics (Summarized from various sources including J. R. Meyer-Arendt, *Introduction to Modern Optics*, Fourth Edition, Prentice Hall, 1994.)

Aberration	Cause and character	Correction
Chromatic aberration	Focal point F depends on λ (n depends on λ). Image blur	Doublet
Monochromatic aberration types		
Spherical	On-axis and off-axis blur	Lens bending; aspherical lenses; gradient index; doublet
Coma	Off-axis blur	Lens bending; spaced doublet with central stop
Astigmatism	Off-axis blur	Spaced doublet with stop
Curvature of field	Off-axis objects imaged onto a curved surface instead of a plane	Spaced doublet. Field flattener
Distortion	Off-axis distortion due to varying magnification with distance from axis	Spaced doublet with stop

it is possible to reduce aberrations to an insignificant level.

Absorption is the loss in the power of an electromagnetic radiation that is traveling in a medium. The loss is due to the conversion of light energy to other forms of energy, e.g. lattice vibrations (heat) during the polarization of the molecules of the medium, local vibrations of impurity ions, excitation of electrons from the valence band to the conduction band, etc.

Absorption broadening see *photon reabsorption broadening*.

Absorption coefficient, α, characterizes the absorption of photons as light propagates along a certain direction in a medium. It is the fractional change in the intensity of light per unit distance along the propagation direction, that is,

$$\alpha = -\frac{\delta I}{I \delta x}$$

where I is the intensity of the radiation. $1/\alpha$ is also the mean probability per unit distance that a photon is absorbed. The absorption coefficient depends on the photon energy or wavelength λ. The absorption coefficient α is a material property. Most of the photon absorption (63%) occurs over a distance $1/\alpha$ and $1/\alpha$ is called the *penetration depth* δ. The absorption coefficient depends on the radiation absorbing processes. If K is the extinction coefficient (imaginary part of the complex refractive index, $N = n - jK$), and λ is the free space wavelength, ω is the angular frequency ($2\pi\nu$), then

$$\alpha = 2(2\pi/\lambda)K = (2\omega/c)K.$$

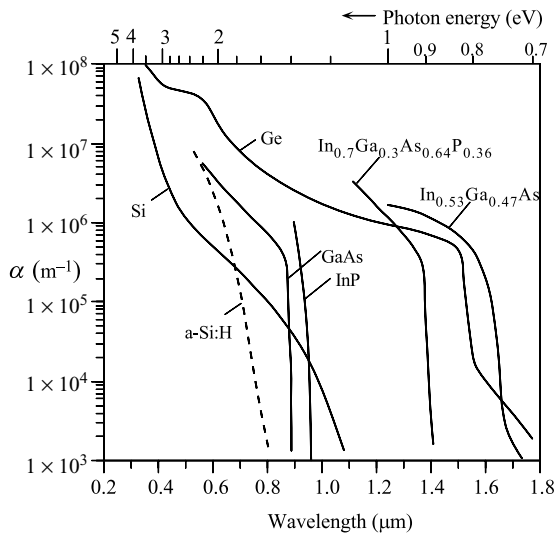

Absorption coefficient (α) vs. wavelength (λ) for various semiconductors. (Data selectively collected and combined from various sources.)

If we know the real and imaginary parts of the relative permittivity, $\varepsilon_r = \varepsilon_{r1} - j\varepsilon_{r2}$, of a medium, we can calculate its α by

$$\alpha = \frac{4\pi}{\lambda}\left[\frac{\left(\varepsilon_{r1}^2 + \varepsilon_{r2}^2\right)^{1/2} - \varepsilon_{r1}}{2}\right]^{1/2}.$$

See *cross-section, sum rules*.

Absorption cross section see *cross-section*.

Absorptivity see *emissivity*.

Acceptance angle, or the *maximum acceptance angle*, is the largest possible light launch angle from the fiber axis. Light waves within the acceptance angle that enter the fiber become guided along the fiber core. If NA is the *numerical aperture* of a step index fiber, and light is launched from a medium of refractive index n_0, then the maximum acceptance angle $\alpha_{\max}$ is given by

$$\sin\alpha_{\max} = \frac{\mathrm{NA}}{n_0} = \frac{\left(n_1^2 - n_2^2\right)^{1/2}}{n_0}$$

where n_1 and n_2 are the refractive indices of the core and cladding of the fiber. The total acceptance angle is twice the maximum acceptance angle and is the total angle around the fiber axis within which all light rays can be launched into the fiber.

Acceptance cone is a cone with its height aligned with the fiber axis and its apex angle twice the acceptance angle so that light rays within this cone can enter the fiber and then propagate along the fiber. See *acceptance angle*.

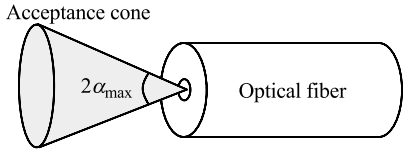

Acceptance cone.

Acceptor atoms are dopants that have one or more less valency than the host atom. They therefore accept electrons from the valence band (VB) and thereby create holes in the VB which leads to a greater hole than electron concentration, $p > n$, and hence to a *p*-type semiconductor.

Achromatic doublet see *chromatic dispersion*.

Achromatic lens is a composite lens (made up of two or more closely fitted lenses) so that the combination has its chromatic aberration corrected at least at two different wavelengths. Stated differently, the achromatic lens has the same focal length f at two wavelengths λ_1 and λ_2 ($>\lambda_1$) and its focal length does not vary significantly with the wavelength from λ_1 to λ_2. For example, a positive achromatic lens usually has a positive (convex) low index lens (e.g. crown glass) and a negative (concave) high index lens (e.g. flint glass) cemented together. The combination is a weaker convex lens.

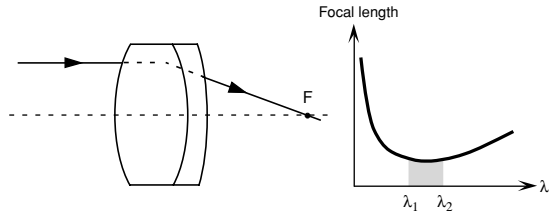

Left: **Achromatic lens** from two lenses. Right: The focal length vs. wavelength behavior.

Achromatic light, see *color*.

Achromatic triplet is a triplet lens that has three lenses to reduce chromatic dispersion. A Steinheim achromatic triplet has a symmetric convex lens of lower refractive index (crown glass) that has higher refractive index (flint) meniscus lenses cemented to its surfaces.

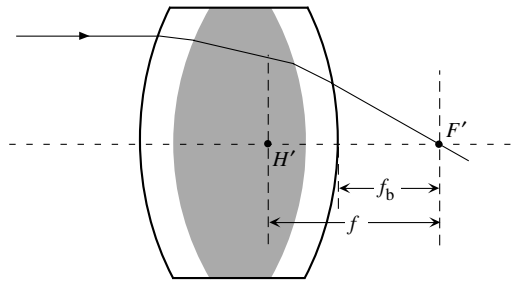

Achromatic triplet f_b is the back focal length measured from the back focal point F' on the lens axis to the lens.

Acoustic velocity see *sound velocity*.

Acoustooptic (AO) modulator makes use of the *photoelastic effect* to modulate a light beam. Suppose that we generate traveling acoustic or ultrasonic waves on the surface of a piezoelectric crystal (such as $LiNbO_3$) by attaching interdigital electrodes onto its surface and applying a modulating voltage at radio frequencies (RF). The *piezoelectric effect* is the phenomenon of generation of strain in a crystal by the application of an external electric field. The modulating voltage $V(t)$ at electrodes will therefore generate a *surface acoustic wave* (SAW) via the piezoelectric effect. These acoustic waves propagate by rarefactions and compressions of the crystal surface region which lead to a periodic variation in the density and hence a periodic variation in the refractive index in synchronization with the acoustic wave amplitude. The periodic variation in the strain S leads to a periodic variation in n owing to the *photoelastic effect*. We can simplistically view the crystal surface region as alternations in the refractive index. An incident light beam will be diffracted by this periodic variation in the refractive index. Depending on the wavelength of the optical (λ) and acoustic waves (Λ), and the length of interaction, there may be a single or multiple diffracted beams. If there are multiple diffracted beams then the AO effect is called *Raman–Nath* diffraction and if there is only the first order, it is referred to as the AO *Bragg diffraction*; the latter is easier to quantify. (See *Raman–Nath diffraction*.) Bragg diffraction occurs at high acoustic frequencies where the acoustic wavelength is short. If the acoustic wavelength is Λ, then the condition that gives the angle θ for a diffracted beam to exist is given by the *Bragg diffraction condition*,

$$2\Lambda \sin\theta = \lambda/n$$

where n is refractive index of the medium, and 2θ is the diffraction (deflection) angle inside the AO diffraction medium, within the device. The intensity of the diffracted beam depends on the power of the acoustic wave that induces the diffraction grating, and hence on the modulating voltage, a convenient way to modulate the intensity of a light beam. If the AO modulator has an essentially first-order diffracted beam, the first-order diffracted intensity I_1 is usually given by

$$\frac{I_1}{I_0} = \sin^2\left[\frac{\pi}{\lambda}\left(\frac{L}{2H}M_2 P_{\text{acoustic}}\right)^{1/2}\right] \approx \frac{\pi^2 M_2 P_{\text{acoustic}} L}{2\lambda^2 H}$$

where I_0 is the zero-order beam, P_{acoustic} is the power in the acoustic wave, M_2 is a figure of merit for the AO medium (given below), L is the acoustic beam length and H the acoustic beam height or width in a plane parallel to the propagation of incident light.

Suppose that ω is the angular frequency of the incident optical wave. The optical wave reflections occur from a moving diffraction pattern which moves with a velocity V_{acoustic}. As a result of the *Doppler effect*, the diffracted beam has either a slightly higher or slightly lower frequency depending on the direction of the traveling acoustic wave. If Ω is the frequency of the acoustic wave then the diffracted beam has a Doppler shifted frequency given by

$$\omega' = \omega \pm \Omega.$$

When the acoustic wave is traveling towards the incoming optical beam, then the diffracted optical beam frequency is up-shifted, i.e. $\omega' = \omega + \Omega$. If the acoustic wave is traveling away from the incident optical beam then the diffracted frequency is down-shifted, $\omega' = \omega - \Omega$. It is apparent that we can modulate the frequency (wavelength) of the diffracted light beam by modulating the frequency of the acoustic waves. (The diffraction angle is then also changed.)

$LiNbO_3$ is a piezoelectric crystal and hence allows the convenient generation of acoustic waves by the simple placement of interdigital electrodes;

Table: Acoustooptic modulator Figures of merit for various acoustooptic materials. N is the refractive index v is the acoustic velocity. (From the Brimstone website and others.)

Material	$LiNbO_5$	TeO_2	Ge	InP	GaAs	GaP	Fused quartz	$PbMoO_4$	Flint glass	Chalcogenide glass
λ (μm)	0.6–4.5	0.4–5	2–12	1–1.6	1–11	0.59–10	0.2–4.5	0.4–1.2	0.45–2	1.0–2.2
n	2.2	2.26	4	3.3	3.37	3.31	1.46	2.26	1.8	2.7
(at μm)	(0.633)	(0.633)	(10.6)		(1.15)	(1.15)	(6.3)	(0.633)		
v km s^{-1}	6.6	4.2	5.5	5.1	5.34	6.3	5.96	3.63	3.51	2.52
M_2	7	35	180	80	104	44	1.6	50	8	164

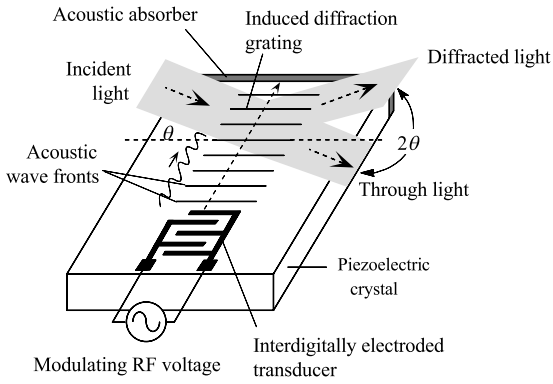

Acoustooptic modulator Traveling acoustic waves create a harmonic variation in the refractive index and thereby create a diffraction grating that diffracts the incident beam through an angle 2θ.

it is used in high-speed IR AO modulators. AO gratings can also be generated in nonpiezoelectric materials because the basic principle is the induction of a diffraction grating by an acoustic wave, which can be coupled into the material from an (external) ultrasonic transducer. The rarefactions and compressions associated with the acoustic wave generates a phase grating by virtue of the photoeleastic effect. For example, germanium is commonly used in various commercially available infrared (2–11 μm) AO devices that deflect light, modulate the light intensity, and shift the optical frequency. AO devices based on other crystals, e.g. TeO_2 (400–1000 nm), GaP (600–1000 nm), $PbMoO_4$ (400–1200 nm) and glasses, e.g. fused silica (240–450 nm), dense flint glass (440–770 nm), chalcogenide glasses (1.2–3 μm), are also available and cover a wide spectral range from UV to IR and implement various AO modulation functions. (Wavelengths in parentheses cover typical useful ranges, and not necessarily the wavelength range of optical transparency.)

The deflection efficiency of an AO modulator depends not only on the material properties such as the efficiency of the optolelastic effect but also on the power in the acoustic wave. One very simple and useful figure of merit M_2 is

$$M_2 = \frac{n^6 p^2}{\rho v^3}$$

where n is the refractive index, p is the photoelastic constant, ρ is the density and v is the acoustic velocity. The n^6 in the numerator implies that the changes in n have the largest effect on the AO modulation efficiency. The modulation speed and hence the bandwidth of an AO is determined by the transit time of the acoustic waves across the light beam waist. If the optical beam has a waist (diameter) d in the modulator, then the rise time (in digital modulation) depends on d/v, which is called the transit time across the beam diameter. Reducing v to increase the speed however results in the reduction of diffraction efficiency so there is a compromise between the speed and diffraction efficiency.

(D. Pinnow, *IEEE Journal of Quantum Electronics*, **6**, 223, 1970.)

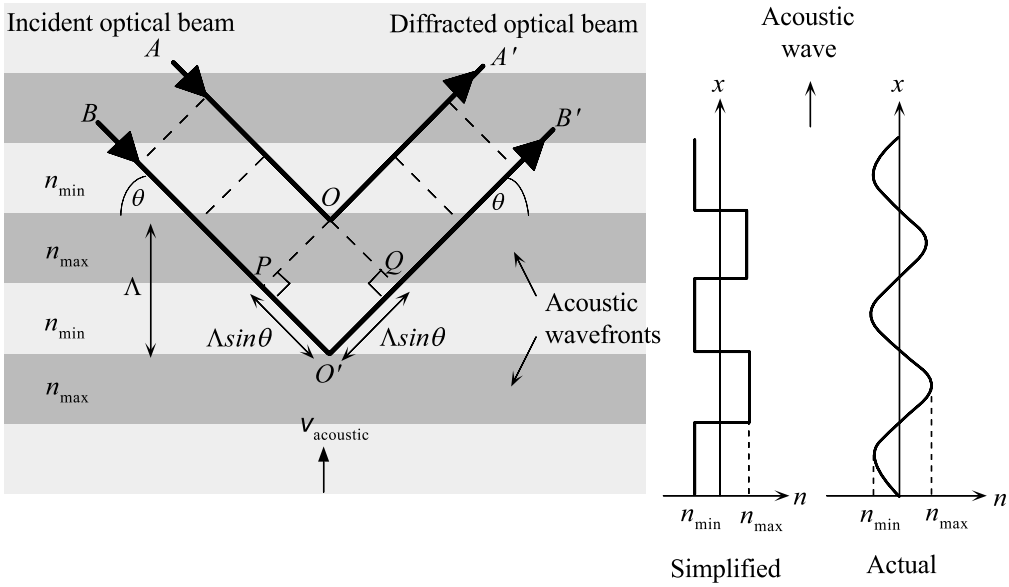

Acoustooptic modulator Consider two coherent optical waves A and B being "reflected" (strictly, scattered) from two adjacent acoustic wavefronts to become A' and B'. These reflected waves can only constitute the diffracted beam if they are in phase. The angle θ is exaggerated (typically this is a few degrees).

Activation energy is the potential energy barrier that prevents a system from changing from one state to another. For example, if two atoms A and B get together to form a product AB, the activation energy is the potential energy barrier against the formation of this product. It is the minimum energy which the reactant atom or molecule must have to be able to reach the activated state and hence be able to form the product. The probability that a system has an energy equal to the activation energy is proportional to the Boltzmann factor: $\exp(-E_A/k_B T)$, where E_A is the activation energy, k_B is the Boltzmann constant and T is the temperature (Kelvins), or it can be expressed as $\exp(\Delta H/RT)$ where ΔH would be in J mole^{-1}, and R is the gas constant.

Activator see *luminescence*.

Active device is a device that exhibits gain (current or voltage or both) and has a directional function. Transistors are active devices whereas resistors, capacitors and inductors are passive devices.

Active region is the region in a medium where direct electron-hole pair (EHP) recombination takes place. For LEDs it is the region where most EHP recombination takes place. In the laser diode it is the region where stimulated emission exceeds spontaneous emission and absorption. It is the region where coherent emission dominates.

Active matrix array (AMA) is a two-dimensional array of pixels in which each pixel has a TFT that can be externally addressed to drive a device such as an LED or a liquid crystal cell located at the pixel; or to read a signal from a sensor located at the pixel. Depending on the application, an AMA can have a few pixels or millions of pixels. The TFT AMA technology was pioneered by Peter Brody using CdSe TFTs in the early 1970s. As shown in the figure, each pixel is identical with its TFT gate

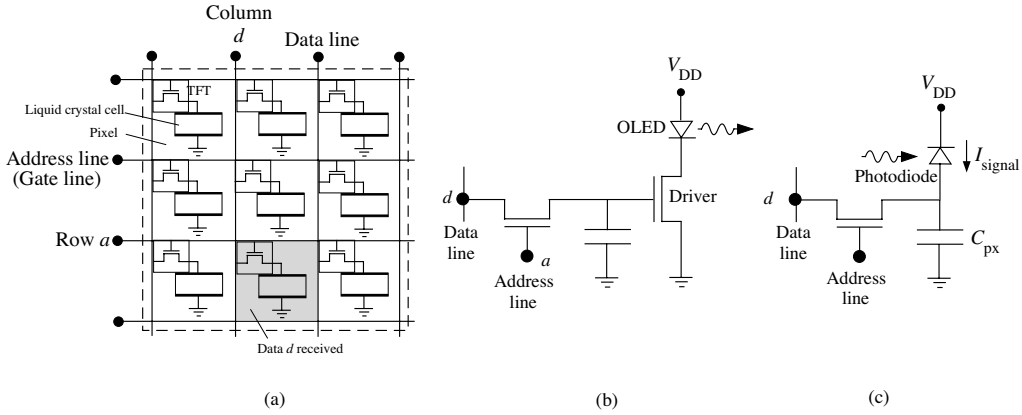

Active matrix array (a) Basic structure of an active matrix array with one TFT transistor in each pixel driving a liquid crystal cell for a liquid crystal display. The gray pixel on row *a* receives the data on data line *d*. (b) A pixel structure that drives an OLED, organic light emitting device (or some other LED with an acceptable current demand). (c) AMA used as a read out array in which a pixel has a photodiode. When light impinges on the pixel photodiode, the photocurrent generated is the signal and is read out at data line *d* by addressing row *a*.

connected to a particular address line and the source to a particular data line. The example in the figure involves an AMA driving an LCD (liquid crystal display), and each pixel has a liquid crystal cell. When a voltage is applied to the address line *a*, each TFT on row *a* is activated. The information as parallel data on the data lines is then transferred to the pixels at row *a*, e.g. column *d* is connected by the TFT to the pixel that crosses *a* and *d*, to pixel *a,d*, which receives the information. Thus, each pixel on row *a* receives its data from the data line. The data has been encoded to activate the liquid crystal cell, to turn it on or off, etc. The address and data lines have drivers, and the whole sequencing of which row is activated is done by a scanning control. One frame of an image in the LCD is generated by scanning one row after another until all the rows have been scanned, i.e. each pixel has received its input signal (data). When the pixel has an LED or an OLED (organic light emitting diode), a second TFT is incorporated as a driver. The AMA can also function to read signals from pixels. In AMA imaging sensors, each pixel has a photodiode. When light impinges on the pixel photodiode, a photocurrent is generated which charges the pixel capacitance. This charge constitutes the signal, and is read out at data line *d* by addressing row *a*. When row *a* is addressed, all signals on that row are read out, that is, the data are read out onto the data lines as *parallel data*, which can be converted into serial data. We scan the whole image row by row (line by line) by starting from the top row and sequentially activating one row after another.

Active matrix sensor see *active matrix array*.

Active pixel sensor (APS) is an active matrix array *image sensor* in which each pixel has two or more transistors, usually CMOS, that provide on-pixel amplification, either providing an actual gain or working as a source follower. In contrast, in a *passive pixel sensor* (PPS) there is no amplification at a pixel; usually a single transistor switch is used to read out the charge. See *active matrix array, CMOS image sensor*.

Add/drop multiplexer (ADM) see *wavelength add/drop multiplexer (WADM)*.

ADU, arbitrary digital units.

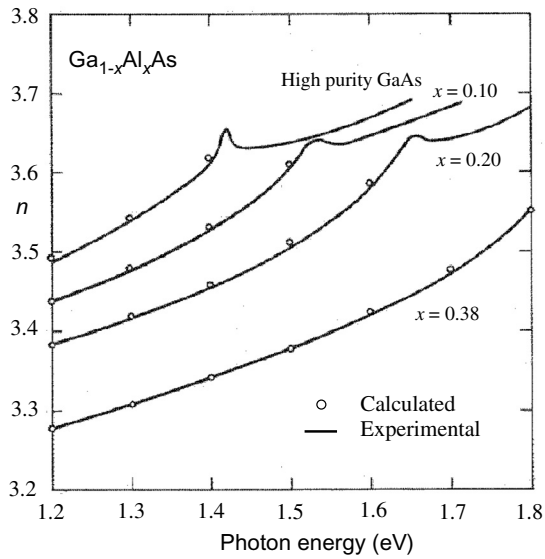

Afromowitz refractive index model Refractive index of $Ga_{1-x}Al_xAs$ as a function of photon energy above the bandgap energy for various compositions x (x is obtained experimentally). Solid curves are experimental n values and the circle points are calculated using the Afromowitz model. (Data from M. A. Afromowitz, *Sold State Communications*, **15**, 59, 1974.)

Afromowitz refractive index model provides a semiempirical method for the imaginary part ε_{r2} of the dielectric constant, and hence for the real part ε_{r1} and thus the refractive index n, of direct bandgap semiconductors as a function of the photon energy $E\,(=h\upsilon)$ when the photon energy is greater than the bandgap energy E_g, and includes three material-dependent constants: E_g (bandgap), E_o (resonant energy) and E_d (oscillator strength or dispersion energy). Usually E_o and E_d are determined experimentally by fitting the calculations to the experimental data. The photon absorption (ε_{r2}) is given by

$$\varepsilon_{r2} = \eta E^4 \quad \text{for } E_g < E < E_f$$

where $\eta = (\pi/2)E_d/[E_o{}^3(E_o{}^2 - E_g{}^2)]$, and $E_f = (2E_o{}^2 - E_g{}^2)^{1/2}$. The real part ε_{r1} can be obtained from the Kramers–Kronig relation as

$$\varepsilon_{r1} = 1 + M_{-1} + M_{-3}E^2 + \frac{\eta}{\pi}\ln\left[\frac{E_f^2 - E^2}{E_g^2 - E^2}\right]E^4$$

in which M_{-1} and M_{-3} are constants (called "moments" of the ε_{r2} spectrum) that depend on E, E_c and E_d as $M_{-1} = (\eta/2\pi)(E_f{}^4 - E_g{}^4)$ and $M_{-3} = (\eta/\pi)(E_f{}^2 - E_g{}^2)$. Once E_g, E_o and E_d are known (are found), ε_{r1} and hence n can be found at any photon energy in the range $E_g < E < E_f$.

Afterglow see *luminescence*.

Air Kerma see *kerma*.

Air mass see *solar radiation*.

Air-mass zero (AM0) radiation see *solar constant*.

Airy disk refers to the central white spot in the *Airy ring* pattern. *Airy rings* represent a diffraction pattern from a circular aperture illuminated by a coherent beam of light. The radius of the Airy disk corresponds to the radius of the first dark ring.

Table: Afromowitz refractive index model Afromowitz model parameters for the refractive index n. E_g represents the direct bandgap energy (sometimes denoted as E_Γ). Data from M. A. Afromowitz, *Sold State Communications*, **15**, 59, 1974.

	$Ga_{1-x}Al_xAs$	$GaAs_{1-x}P_x$	$Ga_xIn_{1-x}P$
E_o	$3.65 + 0.871x + 0.179x^2$	$3.65 + 0.721x + 0.139x^2$	$3.391 + 0.524x + 0.595x^2$
E_d	$36.1 - 2.45x$	$36.1 + 0.35x$	$28.91 + 7.54x$
E_g (or E_Γ)	$1.424 + 1.266x + 0.26x^2$	$1.441 + 1.091x + 0.21x^2$	$1.34 + 0.668x + 0.758x^2$

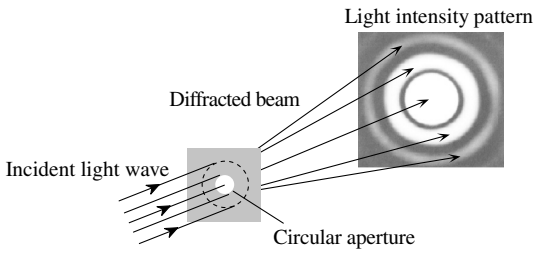

Airy disk A light beam incident on a small circular aperture becomes diffracted and its light intensity pattern after passing through the aperture is a diffraction pattern with circular bright rings (called Airy rings). If the screen is far away from the aperture, this would be a Fraunhofer diffraction pattern.

An *Airy ring pattern* is the Fraunhofer diffraction pattern produced by a circular aperture of diameter D. The circularly symmetric intensity is angularly distributed as

$$I(\theta) = I_0[2J_1(z)/z]^2,$$

where I_0 is the peak intensity, J_1 is the Bessel function of the first order, and $z = (\pi D\theta/\lambda)$. When projected into the focal plane of an imaging instrument with a focal length f, the central spot has a diameter of around $1.22\lambda f/D$. See *diffraction limited system*.

George Bidell Airy (1801–1892, England). George Airy was a Professor of Astronomy at Cambridge and then the Astromer Royal at the Royal Observatory in Greenwich, England. (C. H. Jeens, AIP Emilio Segre Visual Archives, E. Scott Barr and T. J. J. See Collections.)

Airy function is a comb-like, intensity transfer function of a *Fabry–Perot cavity*.

Airy ring pattern see *Airy disk*.

Aliasing is the wrapping or folding back of the high-frequency signal above the Nyquist frequency onto the image as a lower frequency component if the presampling signal has frequency components above the Nyquist frequency, as shown in the figure. Consider a signal $s(x)$ with a spectrum (Fourier transform) $S(f)$ that has no spectral components above f_m. Suppose $s(x)$ is sampled at a sampling frequency (rate) f_s to generate a sampled signal $s_{\text{sampled}}(x)$. The sampled signal spectrum $S_{\text{sampled}}(f)$ has the original spectrum $S(f)$ repeated at every f_s. If $f_s < 2f_m$, there exists an overlapped region in the spectrum of the sampled signal. The frequency band between $(f_s - f_m)$ and f_m is *aliased*, resulting in a distortion of the signal in this frequency band and an exact reconstruction of the signal is not possible. A higher sampling rate or an antialiasing filter can eliminate aliasing. For example, we can use an antialiasing filter to limit the higher spatial frequencies, and reduce f_m until the Nyquist criterion $f_s > 2f_m$ is satisfied and the aliasing is removed. *Aliasing noise* is the image noise associated with the aliasing phenomenon. If aliasing occurs, noise aliasing takes place, any noise component of a frequency higher than the Nyquist or critical frequency (f_c) will be replicated in frequency space and overlap with other noise frequencies in a fashion identical to the overlap of the signal frequencies. The overlapping frequency components of a digital noise power spectrum (NPS) simply add, and this effect potentially increases image noise at frequencies below f_c. Thus, aliasing noise reduces the detective quantum efficiency (DQE) at higher frequencies. See *Nyquist–Shannon theorem, detective quantum efficiency*.

Aliasing noise see *aliasing*.

Aluminum antimonide (AlSb) is an indirect bandgap III-V semiconductor crystal with zinc

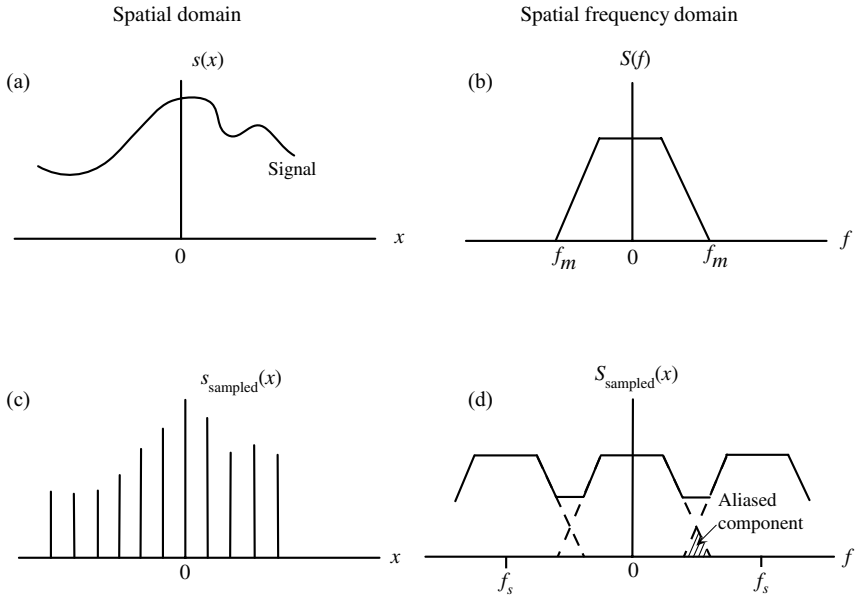

Aliasing (a) and (b): Presampling signal $s(x)$ in the spatial domain, and its Fourier transform $S(f)$ in the spatial-frequency domain, respectively. (c) and (d): Sampled signal $s_{\text{sampled}}(x)$ and its Fourier transform $S_{\text{sampled}}(f)$ in spatial and spatial-frequency domains, respectively.

blende structure having $a = 0.61355$ nm; $\rho = 4.29$ g cm^{-3}; $T_m = 1065$ °C; $\chi = 3.53$ eV; E_g(I) = 1.615 eV (300 K) and E_g(D) = 2.30 (300 K); $\Delta_{so} = 0.673$ eV; $m_{eT}^*/m_e = 0.259$; $m_{eL}^*/m_e = 1.80$; $\mu_e \sim 200$ cm^2 V^{-1}s^{-1}; $\mu_h \sim 400$ cm^2 V^{-1}s^{-1}; ε_r(DC) = 12.04, $\varepsilon_r(\infty) = 10.24$. For $\lambda = 1$ to 20 μm,

$$n = 3.1340 + \frac{0.8032}{\lambda^2} - \frac{0.5166}{\lambda^4} - 0.0004\lambda^2.$$

Aluminum arsenide (AlAs) is an indirect bandgap III-V semiconductor crystal with zinc blende structure: $a = 0.566$ nm; $\rho = 3.76$ g cm^{-3}; $T_m = 1740$ °C; $\alpha_L = 4.9\times10^{-6}$ K^{-1}; $c_s = 0.45$ J g^{-1} K^{-1}; $\kappa \approx 0.91$W cm^{-1} K^{-1}; $\chi = 3.5$ eV; $T_{\text{Debye}} = 446$ K; E_g(I) = 2.168 eV (300K), E_g(I) = 2.230 eV (0K); $\Delta_{so} = 0.30$eV; $m_e^*/m_e = 0.71$; $m_{hh}^*/m_e = 0.76$; $m_{lh}^*/m_e = 0.15$; $n_i < 10$ cm^{-3}; $N_c = 1.5\times10^{19}$ cm^{-3}; $N_v = 1.65\times10^{19}$ cm^{-3}; ε_r(DC) = 10.06, $\varepsilon_r(\infty) = 8.16$; $E_{\text{breakdown}} \approx 5\times10^5$ V cm^{-1}; $\mu_e \sim 300$ cm^{2}V^{-1}s^{-1}; $\mu_h \sim 140$ cm^2 V^{-1}s^{-1}; $D_e \sim 5$ cm^2 s^{-1}; $D_h \sim 5$ cm^2 s^{-1}; $n \sim 3.3$; $\hbar\omega_{\text{op}} = 50$ meV; $B_{\text{radiative}} = 1.8\times10^{-10}$ cm^3 s^{-1}.

Aluminum gallium arsenide ($Al_xGa_{1-x}As$) is a ternary zinc blende semiconductor alloy that is near-lattice matched to GaAs over the entire compositional range with $a = 0.56533 + 0.00078x$ nm; $\rho = 5.32 - 1.56x$ g cm^{-3}; $T_m = 1240 - 58x + 558x^2$ °C; $c_s = 0.33 + 0.12x$ J g^{-1} °C^{-1}; $\kappa = 0.55 - 2.12x + 2.48x^2$ W cm^{-1} °C^{-1}; thermal diffusivity $D_{\text{th}} = 0.31 - 1.23x + 1.46x^2$ cm^2 s^{-1}; $\alpha_L = (5.73 - 0.53x)\cdot10^{-6}$ °C^{-1}, $K = (7.55 + 0.26x)\cdot10^{11}$ dyn cm^{-2}, $G = (3.25 - 0.09x)\cdot10^{11}$dyn/cm^2, $E = (8.53 - 0.18x)\cdot10^{11}$dyn/cm^2, $v = (0.31+0.1x)$, piezoelectric constant of $e_{14} = -0.16-0.065x$ C.m^{-2}, and elastic constants of $C_{11} = (11.88 + 0.14x)\cdot10^{11}$ dyn/cm^2, $C_{12} = (5.38 + 0.32x)\cdot10^{11}$ dyn/cm^2 and $C_{44} = (5.94 - 0.05x)\cdot10^{11}$ dyn/cm^2. The material has a direct bandgap for $x < 0.5$ of E_g (D) ≈ 1.424 + $1.266x + 0.266x^2$ eV, an effective mass for electrons of $(0.063 + 0.083x)m_e$ ($x < 0.45$), density of

(a)

(b)

(c)

Aliasing (a) The original image, roof tops (Italy), where one can clearly distinguish the periodic roof tiles. (b) An undersampled image in which aliasing has introduced significant noise, and the image is not a reconstruction of the original. Many small features are unclear (noisy), edges are jagged, and there is false information. (c) Sampled image with an antialiasing filer. While the higher spatial frequencies have been lost (cut by the filter), the reconstructed image is close to the original with some blurring of very fine details. (Courtesy of Dr. A. S. Mehr, University of Saskatchewan.)

states electron effective mass of $(0.85 - 0.14x)me_o$ ($x > 0.45$), heavy-hole effective mass of $(0.51 + 0.25x)me_o$, and light-hole effective mass of $(0.082 + 0.068x)m_e$. The electron affinity is $4.07 - 1.1x$ eV for $x < 0.45$ and $3.64 - 0.14x$ eV for $x > 0.45$. $T_D = 370 + 54x + 22x^2$ K; ε_r (DC) $= 12.90 - 2.84x$, high frequency $\varepsilon_r = 10.89 - 2.73x$ and the optical phonon energy is $36.25 + 1.83x + 17.12x^2 - 5.11x^3$ meV. The valence band discontinuity for Al_xGa_{1-x} As heterojunctions to GaAs is $\Delta E_v = -0.46x$ eV and that for the conduction band is $\Delta E_c = 0.79x$ eV for $x < 0.41$ and $0.475 - 0.335x + 0.143x^2$ eV for $x > 0.41$. The breakdown field strength is $(4 - 6) \times 10^5$ V cm^{-1}; $\mu_e = 8 \cdot 10^3 - 2.2 \cdot 10^4 x + 10^4 \cdot x^2$ cm^2 V^{-1} s^{-1} for x < 0.45 and $-255 + 1160x - 720x^2$ cm^2 V^{-1} s^{-1} for $x > 0.45$; $\mu_h = 370 - 970x + 740x^2$ cm^2 V^{-1} s^{-1}. The diffusion coefficient D_e for electrons is $200 - 550x + 250x^2$ cm^{2}s^{-1} for $x < 0.45$ and $-6.4 + 29x - 18x^2$ cm^{2}s^{-1} for $x > 0.45$; and $D_h = 9.2 - 24x + 18.5x^2$ cm^{2}s^{-1}. The refractive index n is

$$n^2 = A + \frac{B}{\lambda^2 - C} - D\lambda^2$$

where $A = 13.5 - 15.4x + 11.0x^2$, $B = 0.690 + 3.60x - 4.24x^2$, $C = 0.154 - 0.476x + 0.469x^2$, and $D = 1.84 - 8.18x + 7.00x^2$.

AMA see *active matrix array*.

Amici prism is a prism that provides a deflection through 90° and a flipping of the image.

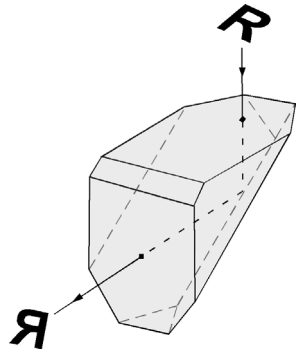

Amici prism.

Amorphous hydrogenated silicon-germanium ($a\text{-}Si_{1-x}Ge_x{:}H$) alloys are amorphous semiconductor alloy films that are prepared by various thin-film fabrication techniques such as chemical vapor deposition (CVD), etc. for use in various optoelectronic applications such as *pin* photodiodes with responsivity in the long-wavelength region; the bandgap decreases with Ge. The Tauc optical gap E_g and the refractive index n are given by

$$E_g(\text{Tauc}) = 1.20 - 0.99x + 0.65x^2$$
$$n = 3.233 + 0.177x + 0.574x^2.$$

See *amorphous semiconductor*.

Amorphous semiconductor is a type of noncrystalline solid that has no long-range periodicity in its structure (crystals have a long-range periodicity) but only short-range order that defines the local chemical binding environment – some short-range order that extends a few atomic spacings. *Hydrogenated amorphous silicon* (a-Si:H) is a noncrystalline form of silicon in which the structure has no long-range order but only short-range order as in the first figure. Each Si atom has four neighbors as in the crystal but there is no periodicity, or long-range order. Without the hydrogen, pure a-Si would have dangling bonds. In such a structure sometimes a Si atom would not be able to find a fourth neighboring Si atom to bond with and will be left with a dangling bond. The hydrogen in the structure (about $\sim$10%) passivates (i.e. neutralizes) the unsatisfied ("dangling") bonds inherent in the noncrystalline structure and so reduces the density of dangling bonds or defects. Amorphous semiconductors do not follow typical crystalline concepts such as Bloch wavefunctions. First, due to the lack of periodicity, we cannot describe the electron as a Bloch wave. Consequently, we cannot use a wavevector k, and hence $\hbar k$, to describe the electron's motion. These semiconductors, however, do have a short-range order, and also possess an energy bandgap that separates a conduction band and a valence band. Window glass has a noncrystalline structure but also has a bandgap, which makes it transparent. Photons with energies less than the bandgap energy can pass through window glass. See *optical absorption in amorphous semiconductors, optical properties of semiconductors*.

The potential energy $V(x)$ of the electron in a noncrystalline structure fluctuates randomly from site to site. In some cases, the local changes in $V(x)$ can be quite strong, forming effective local PE wells (obviously finite wells). Such fluctuations in the PE within the solid can capture or trap electrons, that is, localize electrons at certain spatial locations. A localized electron will have a wavefunction that resembles the wavefunction in the hydrogen atom so that the probability of finding the electron is localized to the site. Such locations that can trap electrons, give them localized wavefunctions, are called *localized states*. The amorphous structure also has electrons that possess extended wavefunctions, that is, they belong to the whole solid. These extended wavefunctions are distinctly different than those in the crystal because they have a very short coherence length due to the random potential fluctuations; the electron is scattered from site to site and hence the mean free path is of the order of a few atomic spacings. The extended wavefunction has random phase fluctuations. The second figure compares localized and extended wavefunction in an amorphous semiconductor. The energy distribution of the density of states (DOS) function, $g(E)$, has defined energies E_v and E_c that separate extended states from localized states. There is a distribution of localized states, called *tail states* below E_c and above E_v. The usual *bandgap* $E_c - E_v$ is called the *mobility gap*. The reason is that there is a change in the character of charge transport, and hence in the carrier mobility, in going from extended states above E_c to localized states below E_c. The electron transport above E_c in the conduction band is dominated by scattering from random potential fluctuations arising from the disordered nature of the structure. The electrons are scattered so frequently

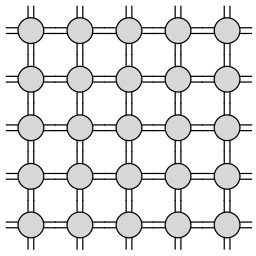

(a) Two-dimensional schematic representation of a silicon crystal

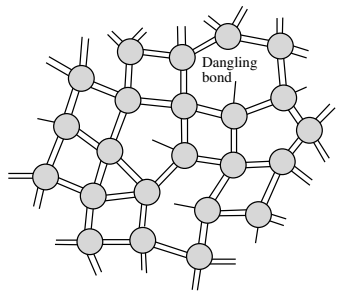

(b) Two-dimensional schematic representation of the structure of amorphous silicon. The structure has voids and dangling bonds and there is no long-range order.

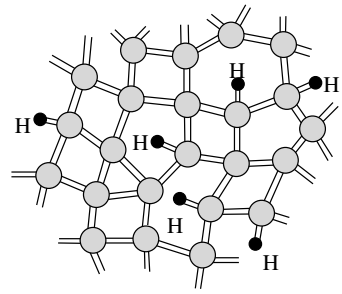

(c) Two-dimensional schematic representation of the structure of hydrogenated amorphous silicon. The number of hydrogen atoms shown is exaggerated.

Amorphous semiconductor Silicon can be grown as a semiconductor crystal or as an amorphous semiconductor film. Each line represents an electron in a bond. A full covalent bond has two lines and a broken bond has one line.

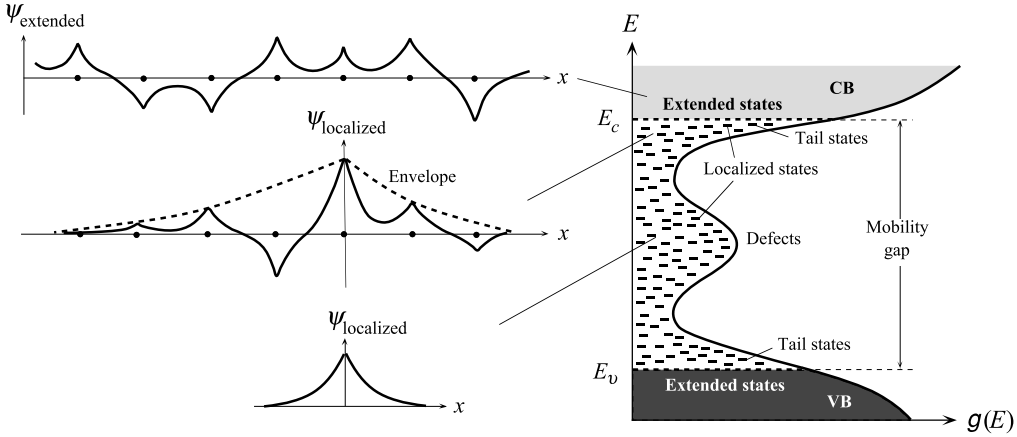

Amorphous semiconductor Schematic representation of the density of states $g(E)$ vs. energy E for an amorphous semiconductor and the associated electron wavefunctions for an electron in the extended and localized states.

that their effective mobility is much less than what it is in crystalline Si: μ_e in a-Si:H is typically 5–10 $\mathrm{cm^2\ V^{-1}\ s^{-1}}$ whereas it is 1400 $\mathrm{cm^2\ V^{-1}\ s^{-1}}$ in a single-crystal Si. Electron transport below E_c, on the other hand, requires an electron to jump, or hop, from one localized state to another, aided by thermal vibrations of the lattice, in an analogous way to the diffusion of an interstitial impurity in a crystal. The electron's mobility associated with this type of hopping motion among localized states is thermally activated, and its value is small. Thus, there is a change in the electron mobility across E_c, which is called the conduction band *mobility edge*. Typically, the conductivity is thermally activated, $\sigma = \sigma_0 \exp(\Delta E_\sigma / k_B T)$. The localized states (frequently simply called

traps) between E_v and E_c have a profound effect on the overall electronic properties. The tail localized states are a direct result of the structural disorder that is inherent in noncrystalline solids, variations in the bond angles and lengths. Various prominent peaks and features in the DOS within the mobility gap have been associated with possible structural defects, such as under- and overcoordinated atoms in the structure, dangling bonds, dopants, etc. Electrons that drift in the conduction band can fall into localized states and become immobilized (trapped) for a while. Thus, electron transport in a-Si:H occurs by multiple trapping in shallow localized states. The effective electron drift mobility in a-Si:H is therefore reduced to about ~ 1 cm^2 V^{-1} s^{-1}. Low drift mobilities obviously prevent the use of amorphous semiconductor materials in high-speed or high-gain otpoelectronic applications. Nonetheless, low-speed electronics is just as important as high-speed electronics in such applications as flat panel displays, solar cells, image sensors, etc. A low-speed flat panel display made from hydrogenated amorphous silicon (a-Si:H) TFTs costs very roughly the same as a high-speed crystalline Si microchip that runs the CPU.

Amorphous semiconductors, optical properties see *optical absorption in amorphous semiconductors*.

Amorphous solid exhibits no crystalline structure or long-range order. It only possesses a short-range order in that the nearest neighbors of an atom are well defined by virtue of chemical bonding requirements. See *glass*, *amorphous semiconductor*.

Amplitude grating see *diffraction grating*.

Amplitude object (especially in microscopy) is an object that alters the amplitude, but not the phase of the transmitted wave with respect to the incident wave; e.g. an absorbing transmission grating, or any thin object with real-valued transmission function. See also *phase object*.

Amplitude-squeezed state see *squeezed states.*

AMS see *active matrix array, image sensor*.

Anamorphic lens is a lens or a lens system that has been designed for applications that involve stronger focusing in one direction than in a perpendicular direction, its extreme case being a cylindrical lens. The magnification is less in one particular lateral lens direction and more in an orthogonal direction, that is the lens squeezes the images in a particular direction. Initially the anamorphic lens was used for horizontally "squeezing" a wide-view image on a film of fixed size (e.g. a 35 mm film); a similar anamorphic lens in the projector expanded the image and restored the original aspect ratio. The anamorphic lens has now found applications in optoelectronics for shaping laser beam profiles emitted by laser diodes that are inherently noncircular. A simple combination of a spherical and a cylindrical lens, or two orthogonally oriented cylindrical lenses, can act as an anamorphic lens system.

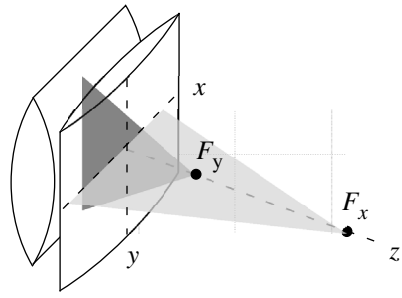

Anamorphic lens A simple anamorphic lens system from two cylindrical lenses; the vertical image (*y*) is squeezed more due to a stronger (shorter focal length) cylindrical lens acting on rays in the *zy* plane.

Anamorphic prism pair is a pair of two identical wedge-type prisms that are aligned and tilted with respect to each other in such a way that an incident beam experiences expansion only in one direction, that is, different magnifications in two orthogonal directions; the pair therefore allows a passing

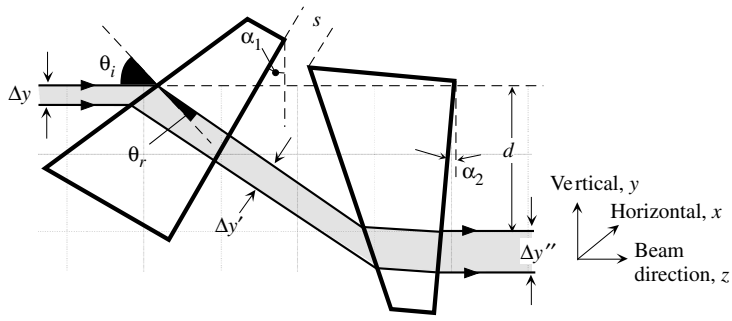

Anamorphic prism pair expands a beam from Δy to $\Delta y''$.

beam's cross-section to be shaped, for example, changed from an elliptical cross-section into circular. The emerging beam from the prism pair is parallel to the incident beam, but displaced by d, which depends on the relative orientations of the prisms and their separation; in practice, typically, d is 5–8 mm. For the prism pair shown, the beam is magnified by $\Delta y''/\Delta y$ vertically (parallel to y) but not horizontally (along x). The angles α_1 and α_2 of the flat faces with the "vertical" determine the anamorphic magnification, i.e. the *magnification aspect ratio* MAR; by changing α_1 and α_2, the anamorphic ratio can be changed from 2:1 to 6:1 quite easily, which allows a highly asymmetrical elliptical beam from a laser diode to be shaped into a circular beam cross-section. For example, for a particular pair of prisms (a Melles Griot anamorphic pair) in which each wedge prism has an apex angle of 29°26′ and, $\alpha_1 = 30.4°$, $\alpha_2 = 0.1°$, then MAR = 3:1, and $d =$ 6.4 mm for light at 830 nm. The anamorphic magnification for each prism, assuming near normal emergence from the flat face, is

$$\begin{aligned}\Delta y''/\Delta y &= \cos\theta_r/\cos\theta_i \\ &= \cos[\arcsin(n\sin\theta_i)]/\cos\theta_i\end{aligned}$$

where Δy and $\Delta y'$ are the incident and deflected beam heights (in the vertical y direction), θ_i and θ_r are the angles of incidence and refraction, and n is the prism material refractive index (normally Schott glass, e.g. SF11). The prism separation s does not affect the MAR but changes the displacement d. Anamorphic prisms are available unmounted or as a mounted pair ready for use.

Angular magnification see *magnifying power, magnification*.

Angstrom (Å) is 10^{-10} meters.

Anisotropy (optical) refers to the fact that the refractive index n of a crystal depends on the direction of the electric field in the propagating light beam. The velocity of light in a crystal depends on the direction of propagation and on the state of its polarization, i.e. the direction of the electric field. Most noncrystalline materials, such as glasses and liquids, and all cubic crystals are *optically isotropic*, that is the refractive index is the same in all directions. For all classes of crystals excluding cubic structures, the refractive index depends on the propagation direction and the state of polarization. The result of optical anisotropy is that, except along certain special directions, any unpolarized light ray entering such a crystal breaks into two different rays with different polarizations and phase velocities. When we view an image through a calcite crystal, an optically anisotropic crystal, we see two images, each constituted by light of different polarization passing through the crystal, whereas there is only one image through an optically isotropic crystal. Optically anisotropic crystals are called *birefringent* because an incident light

Table: Anisotropy (optical) Classification of optical anisotropy in materials, n_o and n_e represent the ordinary and extraordinary wave refractive indices.

Classification	Crystals	Susceptibility	Refractive indices	Examples
Isotropic media	Cubic crystals, liquids, glasses	$\chi_{11} = \chi_{22} = \chi_{33}$	$n_1 = n_2 = n_3 = n_o$	Diamond, glass, fluorite
Uniaxial crystals	tetragonal, hexagonal, trigonal, hexagonal, rhombohedral	$\chi_{11} = \chi_{22} \neq \chi_{33}$ $1 + \chi_{11} = n_o^2$ $1 + \chi_{22} = n_o^2$ $1 + \chi_{33} = n_e^2$	$n_1 = n_2 = n_o$ $n_3 = n_e$ Positive uniaxial $n_e > n_o$ Negative uniaxial $n_e < n_o$	Ice, quartz, calcite, sapphire (Al_2O_3), Lithium niobate ($LiNBO_3$), zircon ($ZrSiO_4$), rutile (TiO_2), sodium nitrate ($NaNO_3$)
Biaxial crystals	orthorhombic, monoclinic, triclinic	$\chi_{11} \neq \chi_{22} \neq \chi_{33}$ $1 + \chi_{11} = n_1^2$ etc.	n_1, n_2, n_3	Mica (muscovite)

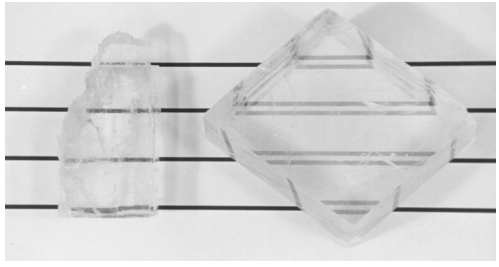

Anisotropy A line viewed through a cubic sodium chloride (halite) crystal (optically isotropic) and a calcite crystal (optically anisotropic).

beam may be doubly refracted. Experiments and theories on "most anisotropic crystals," i.e. those with the highest degree of anisotropy, show that we can describe light propagation in terms of *three* refractive indices, called *principal refractive indices* n_1, n_2 and n_3, along three mutually orthogonal directions in the crystal, say x, y and z, called the *principal axes*. These indices correspond to the polarization state of the wave along these axes. Crystals that have three distinct principal indices also have *two* optic axes and are called *biaxial crystals*. On the other hand, *uniaxial crystals* have two of their principal indices the same ($n_1 = n_2$) and only have one optic axis. Uniaxial crystals, such as quartz, that have $n_3 > n_1$ and are called *positive*, and those such as calcite that have $n_3 < n_1$, are called *negative* uniaxial crystals.

Optical anisotropy in a crystal is related to the polarization **P** in a medium not being in the same direction as the electric field **E** causing it. Suppose that the optical field **E** has components E_x, E_y and E_z along the three principal crystalline axes x, y and z. The induced polarization **P**, with components P_x, P_y and P_z along x, y and z, is then given by a tensor relationship,

$$\boldsymbol{P} = \varepsilon_o \boldsymbol{\chi} \boldsymbol{E} \quad \text{or} \quad \begin{pmatrix} P_x \\ P_y \\ P_z \end{pmatrix} = \varepsilon_o \begin{pmatrix} \chi_{11} & 0 & 0 \\ 0 & \chi_{22} & 0 \\ 0 & 0 & \chi_{33} \end{pmatrix} \begin{pmatrix} E_x \\ E_y \\ E_z \end{pmatrix}.$$

In tensor form, the relative permittivity is $\boldsymbol{\varepsilon}_\mathbf{r} = \mathbf{1} + \boldsymbol{\chi}$, and since $\varepsilon_r = n^2$,

$$\boldsymbol{\varepsilon}_\mathbf{r} = \begin{pmatrix} 1 + \chi_{11} & 0 & 0 \\ 0 & 1 + \chi_{22} & 0 \\ 0 & 0 & 1 + \chi_{33} \end{pmatrix} = \begin{pmatrix} n_1^2 & 0 & 0 \\ 0 & n_2^2 & 0 \\ 0 & 0 & n_3^2 \end{pmatrix}.$$

There are three categories of optical media: isotropic media, uniaxial and biaxial crystals as

summarized in the table. The *optic axis* is taken along the z-axis.

Annealing point of glass is the temperature at which the viscosity of a glass is about 10^{12} Pa s (or 10^{13} dPa s; dPa is decipascals). For example, for fused silica glass this is about 1180 °C. The viscosity of glass is strongly temperature dependent and decreases sharply as the temperature increases. At the annealing point, the viscosity is sufficient to relieve internal stresses.

Anomalous dispersion represents a dispersion behavior, refractive index, n vs. wavelength, λ, in which the refractive index decreases with the frequency of light or n increases with increasing λ. See *refractive index*, *chromatic dispersion.*

Antireflection (AR) coating is a thin dielectric layer coated on an optical device or component to reduce the reflection of light and increase the transmitted light intensity.

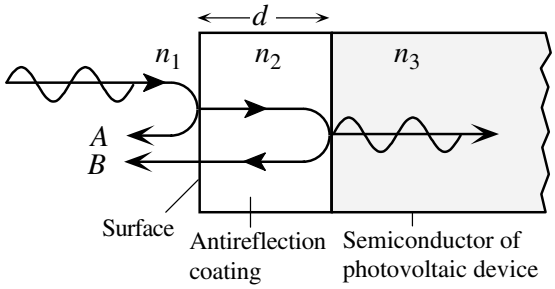

Antireflection coating Illustration of how an antireflection coating reduces the reflected light intensity.

Consider a thin layer of a dielectric material such as Si_3N_4 (silicon nitride) on the surface of a semiconductor optoelectronic device such as a solar cell as shown in the first figure. If this antireflection coating has an intermediate refractive index then the thin dielectric coating can reduce the reflected light intensity. In this case $n_1(\text{air}) = 1$, $n_2(\text{coating}) \approx 1.9$ and $n_3(\text{Si}) = 3.5$. Light is first incident on the air/coating surface and some of it becomes reflected. Suppose that this reflected wave is A. Wave A has experienced a 180° phase change on reflection as this is an *external reflection*. The wave that enters and travels in the coating then becomes reflected at the coating/semiconductor surface. This wave, say B, also suffers a 180° phase change since $n_3 > n_2$. When wave B reaches A, it has suffered a total optical path delay of traversing the thickness d of the coating twice. The phase difference is equivalent to $k_c(2d)$ where $k_c = 2\pi/\lambda_c$ is the wavevector in the coating and is given by $2\pi/\lambda_c$ where λ_c is the wavelength in the coating. Since $\lambda_c = \lambda/n_2$, where λ is the free-space wavelength, the phase difference $\Delta\phi$ between A and B is $(2\pi n_2/\lambda)(2d)$. To reduce the reflected light, A and B must interfere destructively and this requires the phase difference to be π or odd multiples of π, $m\pi$ where $m = 1,3,5, \ldots$ is an odd integer. Thus

$$\left(\frac{2\pi n_2}{\lambda}\right) 2d = m\pi \quad \text{or} \quad d = m\left(\frac{\lambda}{4n_2}\right).$$

Thus, the thickness of the coating must be multiples of the *quarter wavelength* in the coating and depends on the wavelength. To obtain a good degree of destructive interference between waves A and B, the two amplitudes must be comparable. It turns out that we need $n_2 = \sqrt{n_1 n_3}$. When $n_2 = \sqrt{n_1 n_3}$ then the reflection coefficient between the air and coating is equal to that between the coating and the semiconductor. In this case we would need $\sqrt{3.5}$ or 1.87. Thus, Si_3N_4 is a good choice as an antireflection coating material on Si solar cells. Generally an AR coating operates at one or over a narrow range of wavelengths. Further, its effectiveness, the reflectance, depends on the angle of incidence.

The choice of materials is not always the best for a single layer AR coating. *Double layer AR coatings* can achieve negligible small reflections at a specified wavelength. To reduce the reflection of light at the n_1/n_4 surface, two layers n_2 and n_3, each a quarter wavelength (λ/n_2 and λ/n_3) are interfaced between n_1 and n_4 as shown in the second figure.

Table: Antireflection (AR) coating Typical AR materials and their typical (approximate) refractive indices.

	MgF_2	SiO_2	Al_2O_3	CeF_3	Sb_2O_4	Si_3N_4	SiO	ZnS	TiO_2	CdS
n	1.38	1.46	1.65	1.65	1.9–2.1	1.95	2.0	2.35	2.35	2.60

The reflections A, B and C for normal incidence result in a reflectance R given by

$$R = \left[\frac{n_3^2 n_1 - n_4 n_2^2}{n_3^2 n_1 + n_4 n_2^2}\right]^2$$

and R vanishes when

$$(n_2/n_3)^2 = n_1/n_4.$$

Double layer reflectance vs. wavelength behavior usually has a V-shape, and they are called *V-coatings*. Double layer SiN and SiO_2 AR coatings are of particular interest for Si solar cells. Better AR coatings use multiple layers, or coatings that have many layers, each a quarter wave thick, whose refractive index changes from layer to layer forming an *effective graded index* AR coating.

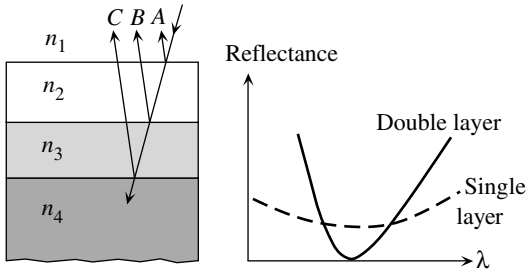

Antireflection coating A double layer AR coating and its V-shaped reflectance spectrum over a wavelength range.

Antistokes shifted scattering see *Stokes shift*.

Aperture is an opening, such as a hole, that allows light from an object to enter the optical or optoelectronic system, usually for detection or imaging.

Aperture function see *Fourier analysis of diffraction*.

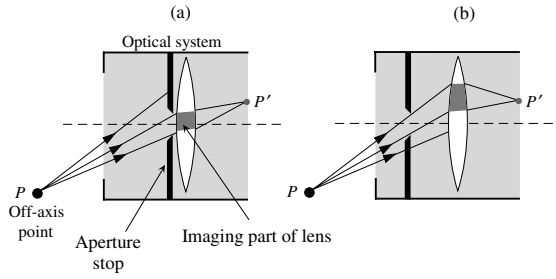

Aperture stop (a) Stop next to lens. Only the central part of the lens is used for imaging an off-axis point P to P'. (b) Stop at a distance from the lens. The outer lens region is used for imaging.

Aperture stop is the major light limiting physical constraint, such as a well-defined hole in an otherwise opaque shield (or the lens holder or retainer itself) that is usually placed on the optical axis and in front of, or behind, a lens in an optical imaging system to prevent marginal rays passing through, or to allow only light rays near the center of the lens to pass through. It is the smallest opening in a lens system, an optical system, through which light has to pass. An aperture stop whose size is adjustable is an *iris diaphragm*. Use of such aperture stops improves the optical performance, though at the expense of image illuminance (brightness); for example, spherical aberration and coma can be reduced by restricting marginal rays. Spherical aberration varies as the cube of the aperture diameter and hence there can be a significant improvement in spherical aberration by using a stop. The placement of the stop, whether right next to the lens or some distance away from the lens, is also important in optical design; the stop-to-lens separation d can affect the magnification of an off-axis object point because different parts of the lens are used for imaging, depending on d, as shown

Table: Aplanatic lens A particular aplanatic lens design that brings a collimated beam to a diffraction-limited focal spot at a back focal length of about 2 mm from the lens. (From M. Mansuripur, *Classical Optics and Its Applications*, Cambridge University Press, 2002). Lens diameter is 4 mm. D is the lens diameter. See figue for other quantities. (NA is numerical aperture. Distances in mm.)

D	t_c	f	R_1	R_2	$h = VH$	n	NA
4	1	2.6733	2.26875	3.87493	0.2894	2.49486	0.75

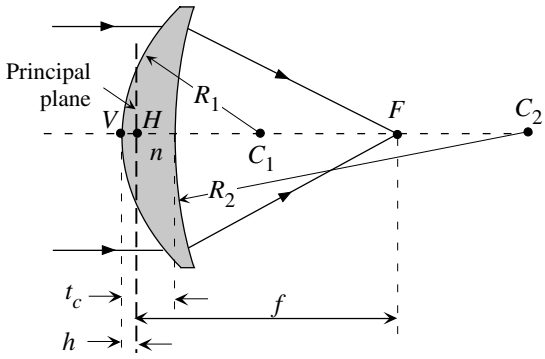

Aplanatic lens that has been designed for an object at far distance.

in the figure. Adjusting the aperture size, the iris diaphragm, in a camera changes the *depth of field*, range of object positions that can be imaged with tolerable (or negligible) blur. A smaller aperture allows a greater depth of field but at the expense of image illuminance.

Aplanatic lens is a meniscus lens (normally a positive or a converging meniscus) that has been shaped to have minimal spherical aberration and coma. Aplanatic lenses are usually aberration optimized for particular applications, such as an object at infinity, etc. since the required radii R_1 and R_2 of curvature of the two lens surfaces for aberrationless imaging depends on the object and image locations. A properly designed aplanatic lens, for example, can bring a collimated beam (parallel rays) to a diffraction-limited spot. The table lists the design characteristics of one such apalanatic lens. The aplanatic lens was invented by the Scottish astronomer Robert Blair (1748–1828). (L. C. Martin, *Proc. Phys. Soc.*, **56**, 104, 1944.)

See *aberrations, Coddington position and shape factors, coma, spherical aberration*.

Aplanatic optical system has been designed to form an image that is free of spherical (on-axis) and coma (off-axis) aberrations. The design of an aplanatic system follows Abbe's sine condition. See *Abbe's sine condition, spherical aberration, coma*.

Aplanatic points are conjugate points P and P' (i.e. object point P and its corresponding image point P') that are on the axis of an optical system, such as a converging lens, that satisfy the *Abbe sine condition*; for a lens, it means that all rays emerging from P that can be captured (and used in imaging) by the optical system converge on P'. The points P and P' are interchangeable in an optical system. The two focal points of an ellipsoidal reflecting surface form aplanatic points, P and P', because all rays from a point source placed at P will be reflected to pass through P'.

Apochromatic lens (apochromat) uses three lenses to eliminate chromatic aberration at three colors or wavelengths; three different colors are focused to the same point by the use of lenses made from three different glasses with different refractive indices. See *chromatic aberration*.

Apodization is a filtering technique mostly used under incoherent light that consists in tailoring the pupil transmittance in such a way that the secondary maxima (the "feet") of the optical transfer function are highly reduced. For instance, one can replace a uniform pupil by a Gaussian-modulated

transmittance. This is often done in astronomy in order to enhance the weakest components of an image. The drawback is a slight loss in resolution.

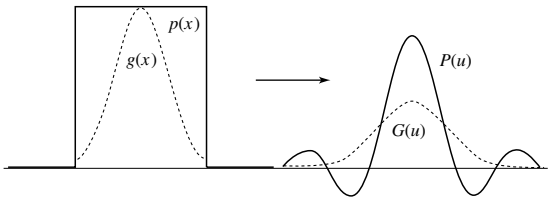

Apodization Typical example of apodization by a one-dimensional Gaussian transmittance $g(x)$, as compared to a uniform pupil $p(x)$. The Gaussian transfer function $G(u)$ appears more regular, albeit slightly larger that the sine-cardinal $P(u)$. $G(u)$ and $P(u)$ are the Fourier transforms of $g(x)$ and $p(x)$.

Arc lamp is a type of gas discharge lamp in which an electric discharge through an arc, an ionized plasma, is maintained between two electrodes. The type of gas or vapor in which the discharge is achieved characterizes the arc. For example, if the gas is xenon, it would be a xenon arc lamp; if it is mercury vapor, it is a mercury vapor arc lamp. (Apparently the first arc was demonstrated by Sir Humphry Davy in 1802 at the Royal Institution in the UK.) The electrodes should be able to withstand high temperatures and wear; typically tungsten (or impregnated tungsten) electrodes are used. Some common types of gases that are used in arc lamps are argon, xenon, neon, krypton, sodium, metal halide, and mercury. The gas between the electrodes needs to be ionized to achieve the arc.

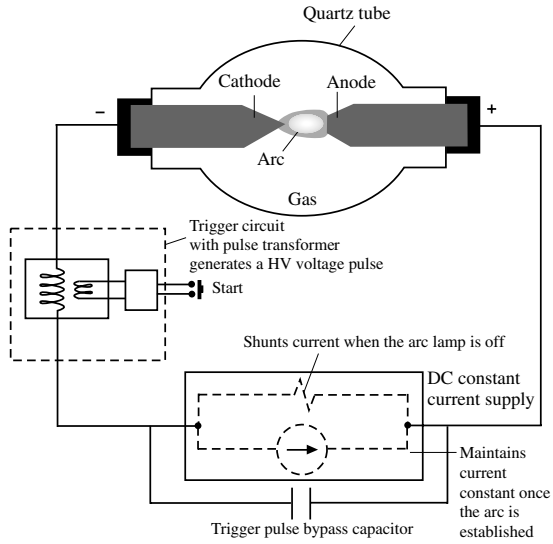

Arc lamp A highly simplified basic schematic sketch of an arc lamp. The cathode has a sharp point to create a large field, and facilitate the discharge. (Various protection electronics not shown.)

The arc is "ignited" or triggered by applying a very high-voltage pulse (several kilovolts) to start the ionization, and once the plasma is initiated and the arc is established, the actual voltage between the electrodes is substantially less than the initial trigger voltage; a circuit with a starter and a ballast controls the initial strike from a high voltage and the subsequent arc current. In steady state operation, the external circuit usually controls the current. The cathode has a sharp point to create a large field, and facilitate the discharge. The advantage of an arc

Table: Arc Lamp Some characteristics of selected arc lamps. Lm/W is the luminous efficacy and quoted values are typical; T_{color} is the color temperature of the source. The spectral ranges are typical values, which also depend on the tube, window and lens materials transmittance.

Arc lamp	Spectral range (nm)	Comment
Xe	200–2000	Bright white source, 15–45 lm/W. Broad spectrum. Light appears white with a $T_{color} \approx$ 6000–6500 K. High-intensity white light applications such as theatre and cinema projectors, stage lighting, etc.
Hg-Xe	200–2000	Similar to the Xe lamp but high UV emission
Hg	200–2000	Good efficacy, 20–50 lm/W. $T_{color} \approx$ 4000–6000 K. Roadways, landscapes, residential and commercial security, parking lots, industrial places, etc.

lamp is that it can provide a broad range of wavelengths from UV to infrared wavelengths; for example, xenon and mercury arc lamps can cover the 180–2000 nm range. The spectrum will also have numerous intense spectral peaks due to the transitions of the excited gas ions. Short arc lamps have their electrodes separated by a very short distance, a few millimeters, and are enclosed in a quartz or fused silica spherical or oblong bulb. They are very convenient in generating high-intensity light. Arc lamps are used in numerous applications as listed in the table: projectors, search lights, floodlights, street and parking lot lighting, display lighting, industrial and commercial places, security areas, UV curing of polymers, and in various scientific and medical instruments and scientific applications such as photochemistry. See *glow discharge lamp, xenon lamp*.

Argon ion laser can provide powerful CW visible coherent radiation of several watts. The laser operation is achieved as follows. The Ar atoms are ionized by electron collisions in a high current electrical discharge. Further multiple collisions with electrons excite the argon ion, Ar^+, to a group of 4*p* energy levels ~35 eV above the atomic ground state. Thus a *population inversion* forms between the 4*p* levels and the 4*s* level which is about 33.5 eV above the Ar atom ground level. Consequently, the stimulated radiation from the 4*p* levels down to the 4*s* level contains a series of wavelengths ranging from 351.1 nm to 528.7 nm. Most of the power, however, is concentrated, approximately equally, in the 488 and 514.5 nm emissions. The Ar^+ ion at the lower laser level (4*s*) returns to its neutral atomic ground state via a radiative decay to the Ar^+ ion ground state, followed by recombination with an electron to form the neutral atom. The Ar atom is then ready for "pumping" again. The Doppler broadened linewidth of the 514.5 nm radiation is about 3500 MHz ($\Delta\upsilon$) and is between the half-intensity points. Typically in the argon-ion laser the discharge tube is made of beryllia (beryllium oxide).

Typical argon ion laser parameters are (From W. T. Silfvast, *Laser Fundamentals, Second Edition*, Cambridge University Press, 2004): laser wavelengths most often used = 488.0 nm; laser transition probability = 7.8×10^7 s^{-1}; upper laser level lifetime = 1.00×10^{-8} s; stimulated emission cross-section = 2.6×10^{-16} m^2; spontaneous emission linewidth and gain bandwidth, FWHM = 2.7×10^9 Hz; population inversion density = 2×10^{15} m^{-3}; small-signal gain coefficient = 0.5 m^{-1}; laser gain-medium length (L) = 0.1–1.0 m; single-pass gain = 1.05–1.65; gas pressure < 0.1 torr; gas temperature, 1200°C; mode of operation is CW; output power = 100 mW to 50 W, TEM_{00} or multimode.

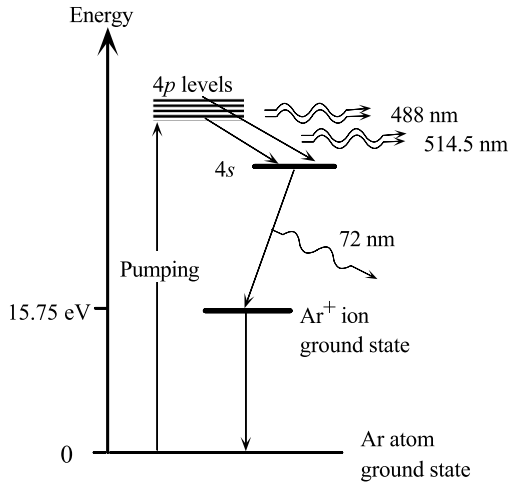

The Ar-ion laser energy diagram

Argon ion laser energy diagram.

Armoring is the protective "cover" made of metal wires or bands that is put around a cable sheath; it provides protection against harsh external environments.

Arrhenius temperature dependence implies that the rate of change in a physical or chemical process, or the particular property under observation, has an exponential temperature dependence of the

form

$$\text{Rate} = C \exp\left(-\frac{\Delta H}{RT}\right) \qquad \text{or}$$

$$\text{Rate} = C \exp\left(-\frac{E_A}{k_B T}\right)$$

where C is a constant, assumed to be relatively temperature independent, R is the gas constant, k_B is the Boltzmann constant, T is the temperature (in kelvins) and ΔH (or E_A) is the activation energy associated with the process, ΔH in J mol^{-1} and E_A in eV atom^{-1} if k_B is expressed in eV K^{-1} atom^{-1}. One good example of the application of the Arrhenius rate equation is the description of the *rate of failure* (R) of electronic devices, which typically follows the above Arrhenius rate equation, at least over a limited temperature range. Accelerated failure tests are carried out at elevated temperatures (e.g. measuring the breakdown voltage of a device) and then the results are extrapolated to the rate of failure at room temperature.

Aspheric lens is a lens that normally has one surface almost flat (or slightly spherical) and the other surface shaped with the right curvature to minimize spherical aberration so that the whole lens area can be utilized for optical applications without suffering significant spherical aberration; "aspherical" implies that the curved surface is not spherical. They are convenient replacements for multielement spherical lens systems that have been designed to be free of spherical aberration. The required curvature is obtained appropriately by molding the lens. In optics, they are frequently used in low *f*-number, high throughput light applications such as condenser lenses in projectors, etc. High-quality glass aspheric lenses can be used to replace multielement microscope objective lenses. Inexpensive molded optical grade plastic aspheric lenses are used in optoelectronics for obtaining collimated light from LEDs. Various aspheric lenses are available for bringing a collimated beam to a nearly diffraction limited focal point. Aspheric lenses in photonics can be used for coupling light into a fiber. Achromatic aspheric lenses correct for both spherical and chromatic aberrations. See *planoconvex lens*.

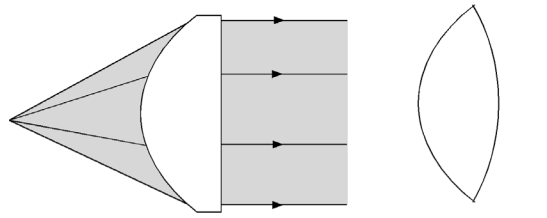

Planoconvex aspheric Biconvex aspheric

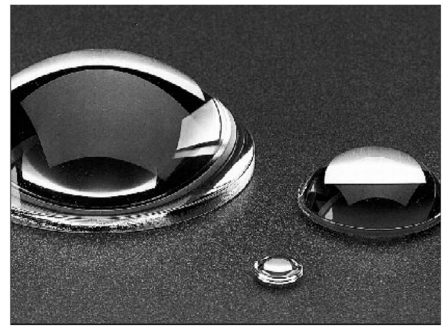

Aspheric lenses (Courtesy of Melles Griot)

Aspheric lens Planoconvex and biconvex aspherical lenses.

Astigmatism is an off-axis lens aberration in which an off-axis object point P is imaged by the lens as a blurred and distorted image due to differently inclined rays from the object not being refracted correctly, as in an ideal lens, to converge to a point (neglecting any diffraction effects). The imaging system is divided into two planes. *The tangential or meridional plane* is the plane that has the optical axis, the principal ray and the object point (P). All rays in this plane are *tangential or meridional rays*. Rays that do not lie in this plane are *skew rays*. The *sagittal plane* is a plane at right angles to the tangential plane; it has the off-axis object point, and the principal ray of the meridional plane. Astigmatism is due to the tangential rays and sagittal rays originating from the same off-axis point object P not producing the same image but rather producing a

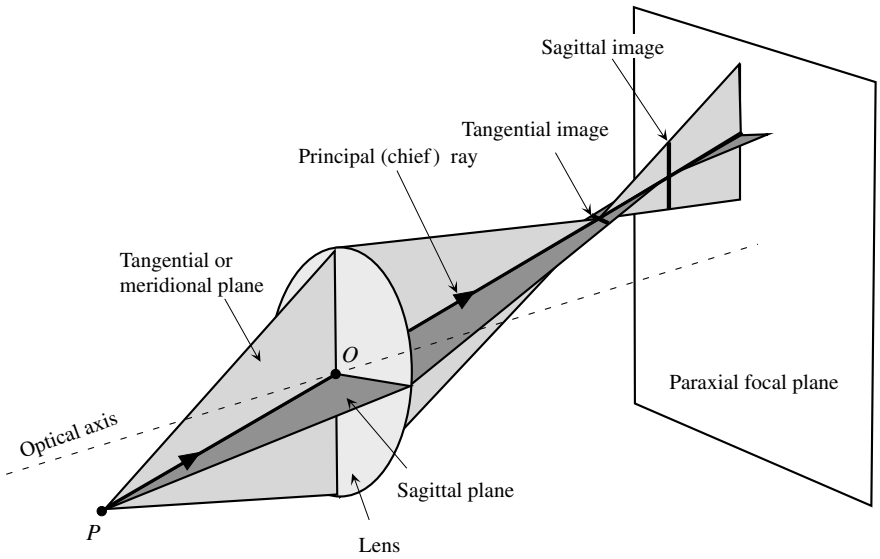

Astigmatism Illustration of astigmatic image from an off-axis point object.

tangential image (a "line" in the sagittal plane) and a sagittal image (a "line" in the tangential plane).

Asynchronous signal is not synchronized to any one time reference signal. Asynchronous transmission does not use a common clock signal between the transmitter and receiver.

Atomic force microscopy see *nanoelectronics*.

Atomic trap see *trapping of atoms*.

Attenuation is the decrease in the optical power of a traveling wave, or a guided wave in a dielectric waveguide, in the direction of propagation due to absorption and scattering. If P_o is the optical power at some location O, and if it is P at a distance L from O along the direction of propagation, then the attenuation coefficient is defined by $\alpha = 10L^{-1}\ln(P/P_o)$. In terms of attenuation measured in decibels

$$\alpha_{dB} = \frac{10}{\ln(10)}\alpha = 4.34\alpha.$$

Attenuation in optical fibers represents the loss in the optical power of a light wave as it propagates along the fiber. It is the fractional decrease in the optical power of a propagating wave per unit length of fiber as it is guided along the fiber. Suppose that the input optical power into a fiber of length L is P_{in} and the output optical power at the end is P_{out}. Then the attenuation coefficient α is

$$\alpha = -\frac{1}{L}\ln\left(\frac{P_{\text{out}}}{P_{\text{in}}}\right).$$

If we know α then we can find P_{out} from P_{in} through, $P_{\text{out}} = P_{\text{in}}\exp(-\alpha L)$. Generally optical power attenuation in a fiber is expressed in terms of decibels per unit length of fiber typically as dB per km. The attenuation of the signal in decibels per unit length is defined in terms of the logarithm to base 10 by

$$\alpha_{\text{dB}} = -\frac{1}{L}\log\left(\frac{P_{\text{out}}}{P_{\text{in}}}\right) \qquad \text{or}$$

$$\alpha_{\text{dB}} = \frac{10}{\ln(10)}\alpha = 4.34\alpha.$$

The first figure shows the attenuation in a typical silica glass-based optical fiber. The sharp increase in the attenuation at wavelengths beyond 1.6 μm in the *infrared* region is due to energy absorption by "lattice vibrations" of the constituent ions of the glass material. There is another intrinsic material absorption in the region below 500 nm, not shown

in the figure, which is due to photons exciting electrons from the valence band to the conduction band of the glass. There is a marked attenuation peak centered at 1.4 μm, and a barely discernible minor peak at about 1.24 μm. These attenuation regions arise from the presence of hydroxyl ions as impurities in the glass structure inasmuch as it is difficult to remove all traces of hydroxyl (water) products during fiber production. The overtone at 1.24 μm is negligible in most modern fibers. There are two important windows in the α vs. λ behavior where the attenuation exhibits minima. The window at around 1.3 μm is the region between two neighboring OH^- absorption peaks. This window is widely used in optical communications at 1310 nm. The window at around 1.55 μm is between the first harmonic absorption of OH^- and the infrared lattice absorption tail and represents the lowest attenuation. This window is used for long-haul communications. It is important to keep the hydroxyl content in the fiber within tolerable levels. There is a background attenuation process that decreases with wavelength and is due to the Rayleigh scattering of light by the local variations in the refractive index. Random fluctuations in the refractive index give rise to light scattering and hence light attenuation along the fiber. Since a degree of structural randomness is an intrinsic property of the glass structure, this scattering process is unavoidable and represents the lowest attenuation possible through a glass medium. Rayleigh scattering process is inversely proportional to λ^4. By proper design, the attenuation window at 1.5 μm may be lowered to approach the Rayleigh scattering limit. The OH^- peak at 1.4 μm has prevented the use of the E-band in optical communications. However, recent developments in fiber manufacturing have almost totally eliminated the water peak as apparent in the α vs. λ characteristic of a newly developed low-water peak fiber by Lucent in the second figure. There are also *bending losses* that arise whenever a fiber is bent. *Microbending loss* occurs typically whenever the radius of curvature of the bend is microscopically sharp, typically less than 0.1−1 mm. Bending losses are normally ignored when the bend radius is more than 100 mm or so. See *Rayleigh scattering, macrobending loss, microbending loss, reststrahlen absorption*.

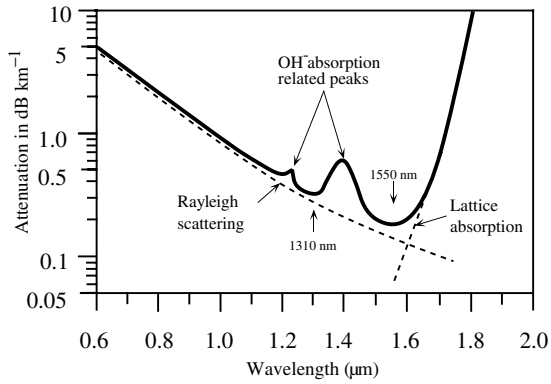

Attenuation in optical fibers Typical attenuation vs. wavelength characteristics of a silica-based optical fiber. There are two communications channels at 1310 nm and 1550 nm.

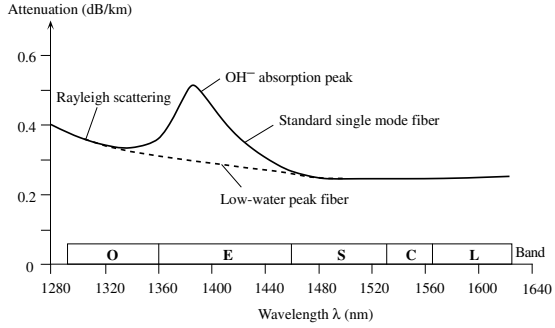

Attenuation in optical fibers Attenuation in a standard single-mode optical fiber and also in a newly developed low water peak fiber. (Lucent; data extracted from A. Lindstrom, *Photonics Spectra*, April 2002, p. 68.)

Attenuation measurement see *cut-back method, insertion loss technique*.

Auger recombination refers to a nonradiative recombination mechanism involving three carriers. Examples include the recombination of

two electrons with one hole, referred to as an ehe process, or two holes with one electron, referred to as ehh process. In an Auger recombination event, the recombination energy from the recombination of an electron and a hole is transferred to the remaining carrier – thus, in the case of an ehe process, the recombination energy is transferred to another electron. The total recombination rate R_{Auger} for ehe and ehh processes can be written:

$$R_{\text{Auger}} = C_{\text{ehe}} n^2 p + C_{\text{ehh}} n p^2$$

where C_{ehe} and C_{ehh} are constants, and n and p refer to the electron and hole concentrations. Clearly, because R_{Auger} depends on the square of carrier density in a given energy band, it only becomes significant at high carrier concentrations – thus, for example, in the case of laser diodes requiring high carrier injection rates to sustain lasing this can be a very significant process. In addition, since the Auger process involves energy transfer to carriers occupying high-lying energy states in the band structure, this process tends to be very sensitive to the details of the semiconductor band structure. In the case of semiconductor heterostructures such as quantum wells, quantum wires and quantum dots, the heterostructure boundaries influence the energy and wavefunctions of carriers, actually increasing the probability of nonradiative Auger recombination. The Auger recombination lifetime τ_{A} can be found from the Auger lifetime τ_{Ai} in an intrinsic semiconductor,

$$\tau_{\text{A}} = \tau_{\text{Ai}} \left(\frac{n_{\text{i}}}{N_{\text{d}}} \right)$$

where n_{i} is the intrinsic concentration and N_{d} is the dopant concentration.

Autocorrelation function, $R(\tau)$, is a function that characterizes the correlation of two points on the same function $x(t)$ that are separated by a time interval τ by integrating the product $x(t)$ and $x(t-\tau)$ over all times

$$R(\tau) = \frac{1}{T} \int_0^T x(t) x(t-\tau) dt \quad \text{as } T \to \infty.$$

$R(\tau)$ is an even function and $R(0)$ represents the average power in the signal if $x(t)$ is a voltage or current. Autocorrelation functions are useful in signal processing, defining coherence in optics, and they can be used to conveniently obtain the spectral power densities of various quantities through the *Wiener–Khintchine theorem*. The autocorrelation function $R(t)$ and the spectral power density $S(f)$ of $x(t)$ form a Fourier transform pair. See *coherence, noise*.

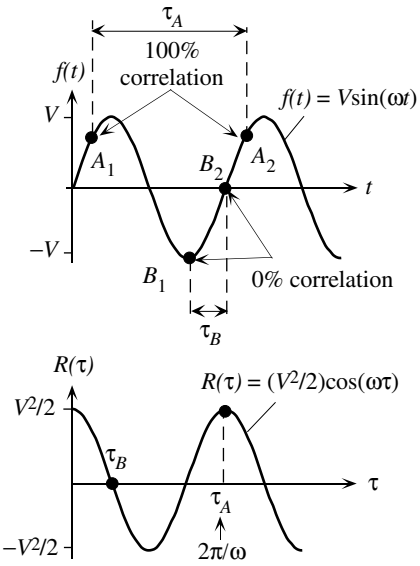

Autocorrelation function A sinusoidal waveform $x(t) = f(t) = V\sin(\omega t)$ and its autocorrelation function $R(\tau)$. While points A_1 and A_2 have 100% correlation (R is maximum), B_1 and B_2 have no correlation ($R = 0$). A_1 and A_2 are points that have the same magnitude, slope and curvature (and higher derivates), whereas this is not the case for B_1 and B_2.

Avalanche breakdown is the enormous increase in the reverse current in a *pn* junction when the applied reverse field is sufficiently high to cause the generation of electron–hole pairs by impact ionization in the space charge layer. See *impact ionization*.

Avalanche multiplication see *impact ionization*.

Avalanche multiplication factor, M, of an avalanche photodiode (APD) is defined as

$$M = \frac{\text{Multiplied photocurrent}}{\text{Primary unmultiplied photocurrent}} = \frac{I_{\text{ph}}}{I_{\text{pho}}}$$

where I_{ph} is the APD photocurrent that has been multiplied and I_{pho} is the primary or unmultiplied photocurrent.

Avalanche noise is the excess noise in the photocurrent of an avalanche photodiode due to the statistics of the multiplication process occurring in the avalanche region. The avalanche process does not occur continuously and smoothly in time but as discrete events whose frequency of occurrence fluctuates in the avalanche region about some mean value. Thus the multiplication M fluctuates about a mean value. The result of the statistics of impact ionization is an excess noise contribution, called *avalanche noise*, to the multiplied shot noise. Suppose that I_{do} is the dark current and I_{pho} is the photocurrent, both in the absence of multiplication, M is the multiplication factor and B is the bandwidth of the detector. Then the noise current in an avalanche photodiode (APD) is given by

$$i_{n-\text{APD}} = [2e(I_{\text{do}} + I_{\text{pho}})M^2 FB]^{1/2}$$

where F is called the *excess noise factor* and is a function of the avalanche multiplication factor M and the impact ionization probabilities (called coefficients). Generally, F is approximated by the relationship $F \approx M^x$ where x is an index that depends on the semiconductor, the APD structure and the type of carrier that initiates the avalanche (electron or hole). For Si APDs, x is 0.3–0.5 whereas for Ge and III–V (such as InGaAs) alloys it is 0.7–1. See *avalanche photodiode, impact ionization, noise, excess noise*.

Avalanche photodiode (APD) is a photodiode with a depletion region in which the field is sufficiently large for an avalanche multiplication of photogenerated charge carriers by impact ionization. The avalanche process in the APD occurs over a limited region of the depletion layer and the photodiode design typically allows only the multiplication of one type of carrier, for example electrons for Si.

Axial or longitudinal modes are allowed electromagnetic stationary waves that exist along the optical cavity length whose electric field patterns are determined by the length L of the optical cavity, e.g.

$$m\left(\frac{\lambda}{2n}\right) = L$$

where λ is the free-space wavelength, n is the refractive index of the cavity medium and m is an integer, $1, 2, \ldots$ Longitudinal modes of an optical cavity are normally associated with transverse modes of the cavity. Each transverse mode has many longitudinal modes.

Axicons are conical lenses which image a point source into a line focus. Some authors describe it as a rotationally symmetric prism. Importantly, such lenses can generate Bessel beams – nondiffracting beams in which the transverse intensity distribution is constant along the direction of propagation. Axicons have been used for precise alignment systems for large telescopes and for scanning systems such as those used in supermarket scanners. The latter systems take advantage of the axicon's large depth of field. An axicon with a spherical lens can focus a collimated laser beam into a ring; the intensity distribution is a ring pattern around the lens axis. Other interesting applications of axicons are in realizing optical traps. The term "axicon" is due to John McLeod (1954) (J. H. McLeod, *J. Opt. Soc. Am.*, **50**, 66, 1960.)

Azimuthal mode number (l) is one of two integers that are normally used to characterize propagating modes in a *step index fiber* (or more generally in a cylindrical waveguide). It characterizes the azimuthal field distribution. In a step index fiber, there are $2l$ maxima in the light intensity around a circle centered on the fiber axis.